The neuropeptides VIP and PACAP inhibit SARS-CoV-2 replication in monocytes and lung epithelial cells, decrease the production of proinflammatory cytokines, and VIP levels are associated with survival in severe COVID-19 patients.

Jairo R. Temerozo[1,10,*], Carolina Q. Sacramento[2,3], Natalia Fintelman-Rodrigues[2,3], Camila R. R. Pão[2], Caroline S. de Freitas[2,3], Suelen da Silva Gomes Dias[2], André C. Ferreira[2,3,4], Mayara Mattos[2,3], Vinicius Cardoso Soares[2,5], Lívia Teixeira[2], Isaclaudia G. de Azevedo-Quintanilha[2], Eugenio D. Hottz[6], Pedro Kurtz[7,8], Fernando A. Bozza[8,9], Patrícia T. Bozza[2], Thiago Moreno L. Souza[2,3], Dumith Chequer Bou-Habib[1,10,*]

[1]Laboratory on Thymus Research, Oswaldo Cruz Institute, Fiocruz, Rio de Janeiro, RJ, Brazil; [2]Laboratory of Immunopharmacology, Oswaldo Cruz Institute, Fiocruz, Rio de Janeiro, RJ, Brazil; [3]National Institute for Science and Technology on Innovation in Diseases of Neglected Populations (INCT/IDPN), Center for Technological Development in Health (CDTS), Fiocruz, Rio de Janeiro, RJ, Brazil; [4]Iguaçu University, Nova Iguaçu, RJ, Brazil; [5]Program of Immunology and Inflammation, Federal University of Rio de Janeiro, UFRJ, Rio de Janeiro, RJ, Brazil; [6]Laboratory of Immunothrombosis, Department of Biochemistry, Federal University of Juiz de Fora (UFJF), Juiz de Fora, Minas Gerais, Brazil; [7]Paulo Niemeyer State Brain Institute, Rio de Janeiro, RJ, Brazil; [8]D'Or Institute for Research and Education, Rio de Janeiro, RJ, Brazil; [9]Evandro Chagas National Institute of Infectious Diseases, Fiocruz, Rio de Janeiro, RJ, Brazil; [10]National Institute for Science and Technology on Neuroimmunomodulation, Oswaldo Cruz Institute, Fiocruz, Rio de Janeiro, RJ, Brazil.

Key words: SARS-CoV-2/COVID-19/VIP/PACAP/Monocytes

Corresponding authors: Jairo R. Temerozo and Dumith Chequer Bou-Habib

Laboratório de Pesquisas sobre o Timo, Instituto Oswaldo Cruz/Fiocruz
Av. Brasil, 4365 - Manguinhos - 21040-360.
Pav. Leonidas Deane/510 - Rio de Janeiro, RJ, Brazil,
Tel. +55 21 3865-8139

E-mail: jairo.jrt@gmail.com, dumith@ioc.fiocruz.br, dumith.chequer@gmail.com

Abstract

Infection by SARS-CoV-2 may elicit uncontrolled and damaging inflammatory response, thus it is critical to identify compounds able to inhibit virus replication and thwart the inflammatory reaction. Here, we show that the immunoregulatory neuropeptides VIP and PACAP were able to inhibit SARS-CoV-2 RNA synthesis in human monocytes and viral production in lung epithelial cells, protect the cells from virus-induced cytopathicity and reduce the production of proinflammatory mediators. Both neuropeptides prevented the SARS-CoV-2-induced activation of NF-kB and SREBP1 and SREBP2, transcriptions factors involved in proinflammatory reactions and lipid metabolism, respectively, and promoted CREB activation in infected monocytes, a transcription factor with antiapoptotic activity and also a negative regulator of NF-kB. VIP levels were elevated in plasma from patients with severe COVID-19, which correlated with the inflammatory marker CRP, viral load, and survival on those patients. Our results provide scientific evidence to further support clinical investigation of these neuropeptides against COVID-19.

Introduction

Individuals with coronavirus disease 2019 (COVID-19), caused by the severe acute respiratory syndrome coronavirus 2 (SARS-CoV-2) [1], may present asymptomatic or mild disease to severe lung inflammation and the life threatening acute respiratory distress syndrome (ARDS) [2,3], besides a variety of extrapulmonary manifestations due to multiple organ infections [4]. Severe SARS-CoV-2 infection is characterized by elevated serum levels of proinflammatory mediators (hypercytokinemia, also known as cytokine storm) such as, for example,

IL-2, IL-6, TNF-α, IL-8, IL-1b, IFN-γ [2,3,5,6]. The dysregulated immune response and production of cytokines and chemokines are hallmarks of SARS-CoV-2 infection and have been pointed as the main cause of the severe lung damage and unfavorable clinical progression of patients with COVID-19 [3–8]. Lately, the in vivo formation of neutrophil extracellular traps (NETs) in the lungs, SARS-CoV-2-induced inflammasome activation and cell death by pyroptosis, have also been considered as risk factors in critically ill COVID-19 patients [9–14].

During the inflammatory response to human pathogenic coronaviruses (hCoVs), circulating neutrophils and monocytes migrate and infiltrate the lungs [15,16] and other organs, where they release toxic amounts of neutrophil extracellular traps [9–12] and proinflammatory cytokines, thus contributing to potentiate and perpetuate the inflammation and eventually exacerbating the tissue damage [17–19]. In fact, it has been reported that SARS-CoV-2 induces neutrophils to release NETs, which are present in the plasma and lungs of critically ill COVID-19 patients, suggesting that they are central components of the exacerbated inflammatory reaction occurring in individuals with COVID-19. Previous studies showed that MERS-CoV- and SARS-CoV-infected macrophages produce high levels of pro-inflammatory cytokines and chemokines [20,21], and, more recently, that lung monocytes from severe pneumonia caused by SARS-CoV-2 are potent producers of TNF-α and IL-6, whose levels were increased in the serum of the same patients [7]. Also, we and other authors have found that SARS-CoV-2 induces inflammasome activation and cell death by pyroptosis in human primary monocytes, either by experimental or natural infection, which are associated with lung inflammation and are risk factors in critically ill COVID-19 patients [13,14].

Thus, it is critical to identify agents able to prevent the infection and concurrently thwart the prototypical dysregulated inflammatory reaction and tissue lesions secondary to SARS-CoV-2 infection. In this work, we evaluated whether the neuropeptides Vasoactive Intestinal Peptide (VIP) and Pituitary Adenylate Cyclase-Activating Polypeptide (PACAP), can present protective effects in SARS-CoV-2 infection. VIP and PACAP share many biological properties through their interaction with the G protein-coupled receptors VPAC1, VPAC2 and PAC1 [22], which are systemically distributed. They have well-characterized regulatory effects on the immune system and anti-inflammatory properties, including control of cell activation and differentiation, down-regulation of inflammatory cytokines and reactive oxygen species and induction of the anti-inflammatory cytokine IL-10 [23–28]. Based on their consistent anti-inflammatory activities, both neuropeptides have been considered as promising therapeutic agents for autoimmune disorders and chronic inflammatory illnesses [29–31]. We report here that VIP and PACAP inhibit SARS-CoV-2 gene replication in human monocytes, viral production in lung epithelial cells, and reduced cellular production of proinflammatory mediators. We also found that VIP levels were elevated in the plasma of individuals with severe manifestations of COVID-19, which correlated with survival on critically ill patients.

Results

VIP and PACAP inhibit SARS-CoV-2 RNA synthesis in human primary monocytes, protecting them from virus-mediated cytopathic effects. Based on our previous findings showing that VIP and PACAP present antiviral effects on HIV-1 infection [32,33], and on their ability to control the inflammatory response, we initially investigated whether both neuropeptides could inhibit viral life cycle in

SARS-CoV-2-infected monocytes. Thus, human primary monocytes were treated with either VIP or PACAP, then infected with SARS-CoV-2 and the replication of viral genome was measured 24 hours later. We found that VIP significantly reduced the SARS-CoV-2 RNA synthesis, achieving 33% and 45% inhibition at 5 nM and 10 nM, respectively (Fig. 1A). PACAP similarly inhibited levels of viral RNA synthesis with 5 nM (40%) and 10 nM (39%) (Fig. 1B). In parallel, we observed that VIP and PACAP, at 10 nM each, completely protected the monocytes from the SARS-CoV-2-mediated cytopathic effect, as measured by the LDH levels in the cell culture supernatant (Fig. 1C). These results show that both neuropeptides are similarly effective in their ability to reduce SARS-CoV-2 genome replication in monocytes and to prevent the virus-induced cell death.

Receptor contribution for the VIP and PACAP mediated inhibition of SARS-CoV-2 replication. Because VIP binds the receptors VPAC1 and VPAC2, and PACAP has high affinity for PAC1, but also binds the VPAC1 and VPAC2 [22], we analyzed the role of the individual receptors in the neuropeptide-mediated inhibition of SARS-CoV-2 RNA replication. To this end, monocytes were treated with specific agonists to VPAC1, VPAC2 and PAC1 (Ala-VIP, Bay 55 9837 and Maxadilan, respectively), and then exposed to SARS-CoV-2. We found that the sole activation of VPAC1 at 1 nM, 5 nM and 10 nM, and of VPAC2 at 1 nM, significantly reduced the SARS-CoV-2 gene replication (Fig. 1D). Of note, the optimal concentrations of the receptor agonists that significantly decreased the SARS-CoV-2 RNA synthesis were similar to those of the natural receptor ligands VIP and PACAP.

We also evaluated if the combination of VIP and PACAP could reduce the viral replication, while reducing the optimal concentration, as VIP and PACAP are reported to act synergistically or in additive fashion in the inhibition of HIV-1 replication in macrophages [32]. We did not observe any increase of viral inhibition activity or reduction of optimal dose when the peptides were combined, being the 10 nM dose the optimal concentration for both peptides, combined or not (Fig. 1E).

Overall, these findings suggest that VPAC1 and VPAC2 receptors are the main contributors for the VIP- and PACAP-mediated SARS-CoV-2 inhibition in monocytes, and that the sole activation of these receptors can lead to a diminished viral inhibition similar as that induced by the own neuropeptides.

VIP and PACAP inhibit SARS-CoV-2 replication in Calu-3 cells and protect them from virus-mediated cytopathic effects. We next evaluated whether VIP and PACAP could also be able to restrict the virus production in pulmonary cells, one of the major targets of SARS-CoV-2. Thus, Calu-3 cells, a lineage of epithelial lung cells highly susceptible to this virus, were infected with SARS-CoV-2 and treated with a range of concentrations of either peptide. We found that VIP decreased the productive infection, reaching 40% and 30% inhibition with 1 nM and 5 nM, respectively (Fig. 2A). PACAP also diminished virus production by 35% and 40% at concentrations equivalent to 10 nM and 50 nM (Fig. 2B). The different optimal concentrations between VIP and PACAP in their ability to control the viral productive infection in Calu-3 cells might be explained by the relative abundance of the neuropeptide receptors, since it has been shown that these cells express only VPAC1 [34]. However, all three receptors are reported to be expressed in lungs, with some studies showing that VPAC1 levels are much higher than VPAC2 (the

other VIP receptor) or PAC1 (to which PACAP binds with higher affinity than to VPAC1 and VPAC2 [22,35–37]). Likewise what we found for monocytes, VIP and PACAP also protected Calu-3 cells from the SARS-CoV-2-induced cytopathogenic effects, at the same optimal viral inhibitory concentrations (1 nM and 50 nM, respectively) of each neuropeptide (Fig. 2C). Using agonists for VIP and PACAP receptors we also verified that VPAC1 is the main receptor involved the inhibition of SARS-CoV-2 in Calu-3 cells, emulating the level of inhibition achieved with VIP, while the exposure to a VPAC2 agonist resulted in a more modest inhibition (Fig. 2D). The stimulus with a PAC1 agonist had no effect on viral replication (Fig. 2D).

Given that monocytes and epithelial cells can be in close proximity in the lungs, and, thus, can interact and exchange molecules, we investigated whether conditioned medium (CM) obtained by SARS-CoV-2-infected monocytes exposed to VIP or PACAP could repress the viral production in human lung cells. While the transference of CM from uninfected monocytes, treated or nor with either neuropeptide, did not modify the virus growth, the addition of CM (at 50% vol/vol – the combination of fresh medium at this ratio did not alter the basal replication of SARS-CoV-2 in Calu-3 cells, Fig. 2E) from infected monocytes increased viral replication 33% when compared to cells maintained with the equivalent combination of fresh media (Fig. 2E). However, when infected Calu-3 cells were exposed to CM from infected monocytes treated with VIP or PACAP, we observed a reduction of 30% and 21% in SARS-CoV-2 replication in these cells (Fig. 2E). This finding raises the hypothesis that both neuropeptides, besides inhibiting the SARS-CoV-2 gene replication, induce monocyte production and release of factors endowed with antiviral activity, which may increase the resistance of neighboring cells to SARS-CoV-2 growth. This bystander effect can reduce viral propagation,

thus eventually protecting the tissues from lesions secondary to SARS-CoV-2-replication and dissemination. Future studies are needed to identify the nature of these putative soluble factors.

Influence of peptidases on VIP and PACAP inhibition of SARS-CoV-2 replication in pulmonary cells. Lung cells are known to express several peptidases [38–40], whose interaction with VIP and PACAP on the cell membrane could modulate the effects of these neuropeptides, favoring or hindering the SARS-CoV-2 replication inhibitory effect. Thus, we evaluated the inhibitory potential of VIP and PACAP in SARS-CoV-2-infected Calu-3 cells in the presence of Bestatin, an inhibitor of several aminopeptidases, including aminopeptidase N, which also acts as receptor for the human coronavirus E229 [41], but not for SARS-CoV-2 [42]. While Bestatin alone (500 nM) did not change the virus yield (Fig. 3A), we verified a gain of effect of VIP at 0.5 nM and 10 nM when combined with Bestatin, (Fig. 3B). Moreover, PACAP achieved an optimal inhibitory concentration at 5 nM when combined with Bestatin, a dose ten-times lower than its optimal inhibitory concentration when alone (50 nM) (Fig. 3C). This result suggests that VIP and PACAP could be targeted by some of the peptidases expressed in pulmonary cells, thus requiring a high concentration to inhibit SARS-CoV-2 replication in these cells.

Association with antivirals increments the neuropeptide anti-SARS-CoV-2 effect in pulmonary cells. Given the enhancement of PACAP-mediated SARS-CoV-2 inhibition when in the presence of a protease inhibitor, we tested whether the association of the neuropeptides with the protease-targeting antivirals could also increase VIP and PACAP inhibition of SARS-CoV-2 replication in pulmonary

cells, as several viral protease inhibitors can also target cell proteases and peptidases [43]. We tested the combination of VIP or PACAP with atazanavir, a classical HIV-1 protease inhibitor which also inhibits SARS-CoV-2 [44], or with ritonavir (whose aminopeptidase inhibition is more prominent than atazanavir [43]). For comparison, we also evaluated the combination with remdesivir, an inhibitor of RNA-dependent RNA polymerase and potent inhibitor of SARS-CoV-2 replication in vitro [45]. The concentrations used for atazanavir (ATV) and ritonavir (RDV) were 5 uM, which did not significantly inhibit SARS-CoV-2 replication (Fig. 4A). The combination the neuropeptides with ATV, did not promote any increment in the inhibition of SARS-CoV-2 replication (Fig. 4B and 4C). However, when in combination with RTV, VIP and PACAP performed better than alone, with a higher inhibition with VIP+RTV at 5 nM than VIP alone at the same concentration; and PACAP achieving an optimal inhibitory concentration of 5 nM (Fig. 4C), equal to that observed when combined to Bestatin (Fig. 3C). Surprisingly, the association of VIP or PACAP with remdesivir (RDV) resulted in a strong potentiation of VIP and PACAP inhibition of SARS-CoV-2 replication in Calu-3 cells (Fig. 4B and 4C).

VIP and PACAP reduce production of proinflammatory cytokines by SARS-CoV-2-infected monocytes and Calu-3 cells. Given the hypothesis that controlling the production of proinflammatory cytokines may be critical for reducing SARS-CoV-2 replication and limiting tissue damages, and based on evidence that VIP and PACAP can regulate the inflammatory response [27,46], we next evaluated whether both neuropeptides could attenuate the production of proinflammatory mediators by SARS-CoV-2-infected monocytes or lung epithelial cells. As shown in Fig. 5A, SARS-CoV-2-infected monocytes produced large amounts of the proinflammatory mediators IL-6, IL-8, TNF-α and MIF relative to uninfected cells

(15, 4, 12 and 18 times more, respectively). In contrast, the treatment of monocytes with either neuropeptide after SARS-CoV-2 infection reduced to 66%, 50%, 66% and 50% the cellular production of IL-6, IL-8, TNF-α and MIF, respectively. Furthermore, VIP and PACAP reverted by approximately the same degree the release of IL-6 and IL-8 by Calu-3 cells (Fig. 5B), implying that VIP and PACAP may offer a critical protection to inflamed lungs affected by SARS-CoV-2 replication. Because proinflammatory cytokines may favor SARS-CoV-2 replication, which, in turn, can amplify the cellular synthesis of these mediators, these findings may support our assumption that VIP and PACAP offer tissue protection by inhibiting virus replication and regulating the boost of cytokine production.

VIP and PACAP regulate the activation of transcription factors in SARS-CoV-2-infected monocytes. Based on the fact that the transcription factor NF-kB is critically involved in the cellular production of inflammatory mediators [47], and on our own findings that VIP and PACAP can inhibit its activation in HIV-1-infected macrophages [33], we investigated whether both neuropeptides would exert this same effect on SARS-CoV-2-infected monocytes. As can be seen in Fig. 6A, we initially observed that NF-kB is up-modulated in infected cells (as measured by the increased amount of phosphorylated NF-kBp65 subunit) and, in addition, that VIP and PACAP reduced the NF-KBp65 phosphorylation, evidencing the significant anti-NF-kBp65 activity of VIP and PACAP. We believe that the SARS-CoV-2-induced NF-kB activation could have contributed for the elevated production of proinflammatory cytokines by SARS-CoV-2-infected monocytes, and that the inhibition of this transcription factor by VIP and PACAP was critical for the decreased synthesis of these mediators by the same cells. Following, we analyzed

the effects of both neuropeptides on the activation of CREB, a transcription factor induced by several GPCR ligands, including VIP and PACAP [48], and also involved in the induction of anti-inflammatory cytokines [49,50]. CREB and NF-kB share the CREB-binding protein/p300 (CBP/p300 protein) as a cofactor, and CREB activation results in the inhibition of NF-kB [51]. We found that activation of CREB was diminished in SARS-CoV-2-infected monocytes, a finding coherent with NF-kB activation in the same cells (Fig. 6B). Consistent with this finding, VIP and PACAP promoted CREB activation (as measured by augmentation of CREB phosphorylation) in those infected monocytes, a result matching the inhibition of NF-kB and the reduction of cellular production of proinflammatory cytokines.

We also evaluated in SARS-CoV-2-infected monocytes the expression of the active form of SREBP-1 and SREBP-2, a transcription factor that also interacts with CBP/p300 [52], and is crucial for the replication of several viruses, including coronaviruses [53–55]. In fact, we and other authors reported that SARS-CoV-2 infection promotes the activation of SREBP, and that this activation is associated with enhanced viral replication [56] and COVID-19 disease severity[57]. We found that the levels of both isoforms of SREBP in active state are increased in SARS-CoV-2-infected monocytes, but reduced in infected monocytes exposed to VIP and PACAP when compared to the untreated infected cells, lowering to the same basal levels found in uninfected monocytes (Fig. 6C and 6D, Supp. Fig. 1).

Together, these results suggest that the restriction of SARS-CoV-2 replication in monocytes and, possibly, in pulmonary cells (represented in this work by the Calu-3 cell line) by VIP and PACAP can also be the outcome of the intrinsic modulation of transcription factors related to the regulation of inflammatory factors that are involved directly and indirectly with the viral replication, either by

244 favoring the cellular damage, through exacerbating the inflammation, or by
245 promoting a permissive cellular microenvironment for viral replication.

246 **Plasma levels of VIP are elevated in patients with severe forms of COVID-19.**
247 Based on our results showing that VIP and PACAP, besides inhibiting viral
248 replication and production, can also control the production of proinflammatory
249 mediators by SARS-CoV-2-infected monocytes and lung epithelial cells, we
250 measured the levels of both neuropeptides in plasma samples of SARS-CoV-2-
251 infected individuals. We found that the amount of VIP is significantly elevated in
252 patients affected by the most severe forms of infection, relative to levels of
253 uninfected healthy controls and asymptomatic/mild patients (Fig. 7A). We also
254 observed that some critically ill patients had increased levels of PACAP, but
255 without statistical significance when considering the entire group (Fig. 7B). In
256 addition, levels of VIP positively correlated with levels of C-reactive protein (CRP)
257 (Fig. 7C), but neither VIP nor PACAP levels correlated with other inflammatory
258 markers, such as D-dimer, fibrinogen or IL-6 (data not shown), or with each other
259 (Fig. 7D). We found a positive correlation between VIP levels and viral load in
260 positive swab samples from mild and severe COVID-19 patients (Fig. 7E and 7F).
261 Severe COVID-19 patients admitted to the ICU were further stratified between
262 those requiring invasive mechanical ventilation or noninvasive O_2
263 supplementation, or according to the 28-day mortality outcome as survivors or
264 non-survivors. For PACAP we did not observe statistical significance in the
265 stratified groups (Fig. 7G and 7H), the same for VIP considering respiratory
266 support (Fig. 7I). However, we found that VIP plasma levels were significantly
267 higher in survivors than in non-survivors (Fig. 7J).

Taking into account that VIP and PACAP regulate inflammatory reactions, it is possible that their increased circulating amounts reflect a counter-regulatory effect elicited by the dysregulated immune response typical of the more severe clinical status of COVID-19 patients. The levels of VIP and PACAP in SARS-CoV-2-infected tissues should be a matter of future studies, to support our hypothesis.

Discussion

In this work, we report that the neuropeptides VIP and PACAP, endogenous molecules presenting anti-inflammatory properties, are able to inhibit SARS-CoV-2 RNA synthesis and viral production and reduce the exacerbated synthesis of proinflammatory mediators due to infection, in human monocytes and lung epithelial cells. Also, we identified that VIP plasma levels are elevated in patients with severe forms of COVID-19, corresponding with viral load, and elevated VIP levels at ICU admission predicts patients' favorable outcome, including association with patient survival. Our findings provide the scientific basis for clinical trials with VIP (Aviptadil), which can be used in intravenous [58] and inhaled [59] formulations. Indeed, first results of clinical studies with VIP are expected to be disclosed in the next year [58,59]. Clinical data, along with mechanism described here, may allow additional larger trials with VIP, an overlooked molecule associated with antiviral, anti-inflammatory and enhanced survival activities.

Both neuropeptides regulate the inflammatory response due to their ability to decrease the production of proinflammatory mediators, and to elicit the production of anti-inflammatory molecules, Given that VIP and PACAP and their receptors are systemically distributed, including the lungs [22,60], brain and gut, we believe that the anti-SARS-CoV-2 effects of both neuropeptides would not be

292 restricted to the respiratory tract, as shown by many studies in other chronic
293 inflammatory illnesses.

294 Here, we initially observed that VIP and PACAP decreased the genome
295 replication of SARS-CoV-2 in monocytes, in parallel with protecting the cells from
296 virus-induced cytopathicity. By diminishing the intracellular levels of viral RNA and
297 other viral molecules, VIP and PACAP could prevent the cell death by pyroptosis,
298 which has been described as one of the main causes of cell damage during
299 SARS-CoV-2 infection [13,14]. While preserving the viability of monocytes, VIP and
300 PACAP also diminished the production of the proinflammatory cytokines IL-6, IL-8,
301 TNF-α and MIF by these cells, which is in agreement with the reported ability of
302 these neuropeptides to regulate the inflammatory response [24–27,61]. We found
303 similar results with lung epithelial cells, further supporting the assumption that VIP
304 and PACAP may offer a critical protection to inflamed lungs affected by SARS-
305 CoV-2 replication. Because these mediators are elevated in patients with COVID-
306 19, it is possible that the higher amounts of VIP in patients with severe forms of
307 infection may reflect a counter-regulatory feedback elicited by the dysregulated
308 immune response of these patients. Interestingly, the cellular protection conferred
309 by VIP or PACAP to SARS-CoV-2-infected monocytes can be transferred to other
310 neighboring virus target cells (Fig. 2E), suggesting that a bystander effect can
311 ultimately protect other SARS-CoV-2-infected cells not directly interacting with VIP
312 or PACAP. More investigations are needed to identify the nature of the putative
313 protecting factors present in the monocyte supernatants.

314 The ability of VIP and PACAP to inhibit the SARS-CoV-2-induced activation
315 of the subunit p65 of the transcription factor NF-kB, pertain to a complex molecular

316 mechanism leading to reduction of proinflammatory cytokines synthesis by SARS-
317 CoV-2-infected monocytes. Also, we detected here that the transcription factor
318 CREB, which can act as a negative regulator of NF-kB [62,63], is down-regulated in
319 SARS-CoV-2-infected monocytes, in opposition to NF-kB activation in the same
320 cells. In some models [64–69], CREB activation is related to induction of anti-
321 inflammatory cytokines concomitant with reduction of pro-inflammatory molecules,
322 mainly through direct transcription of its targets, such as IL-10, or through
323 competing with NF-kB by their shared co-activator protein CBP/p300 [49,62,63,69].
324 Besides its role in the balance between pro- and anti-inflammatory cytokines,
325 CREB activation is also involved with the anti-apoptotic response in monocytes
326 and macrophages, during differentiation and inflammatory stimuli [70,71]. Thus, the
327 imbalance between CREB and NF-kB, either as a direct effect of infection by
328 SARS-CoV-2 or a consequence of exposure of bystander cells to viral products
329 and inflammatory molecules, could be an important target for inhibition of SARS-
330 CoV-2 deleterious effects, at least in monocytes and probably also in lung cells, as
331 a similar imbalance between CREB and NF-kB was observed in an acute
332 inflammatory pulmonary condition [51].

333 The induction of SREBP activity by SARS-CoV-2 was consistent with data
334 showing its increase and association with COVID-19 severity in patients [57].
335 SREBPs are transcription factors that have well-defined roles in the regulation of
336 cellular lipid homeostasis [72]. They exist in an inactive form associated to the
337 endoplasmatic reticulum, where initial activation occurs, completing the activation
338 in the Golgi apparatus before migrating to the nucleus [72]. SREBP1 regulates the
339 expression of fatty acid biosynthesis genes, whilst SREBP2 regulates genes
340 involved in cholesterol biosynthesis, intracellular lipid movement and lipoprotein

import [72]. While crucial for metabolic homeostasis, both transcription factors are involved in pathologies when misbalanced or overactivated [72], and several viruses are reported to induce their activation, as for their optimal replication, the up-regulation of host lipid biosynthesis is a requirement [53–55]. In fact, our group just reported that SARS-CoV-2 activates SREBP-1 and other pathways of lipid metabolism in human cells, and that lipid droplets enhance viral replication and production of inflammatory mediators [56]. The inhibition of SREBP activation in SARS-CoV-2-infected monocytes exposed to VIP and PACAP points to a possible mechanism of viral inhibition directly related to the replicative cycle, since inhibiting SREBPs activation, the replication process can be restrained via limiting the supply of energy and building blocks, ultimately delaying or even stopping the replicative process.

Similar to NF-kB and CREB, the association of SREBP with CBP/p300 [52] makes its function susceptible to the availability of this co-factor, which abundance can be low or high depending on the state of activation of NF-kB and CREB. Thus, the modulation of each one of these factors by VIP and PACAP can reflect a fine tuning of the transcriptional regulation of metabolic and inflammatory pathways, which in turn can affect the replication of SARS-CoV-2.

Because VIP and PACAP signaling pathway outcome is dependent of the combined action of the receptors activated by them (VIP and PACAP receptors can elicit cell signaling in homo and hetero dimers [73]), we evaluated whether they were involved in the final outcome analyzed. Our assays suggest that signaling through the receptors VPAC1 and VPAC2 contributed for VIP- and PACAP-mediated reduction of SARS-CoV-2 RNA synthesis in monocytes and viral

production in Calu-3 cells, with VPAC1 activation alone being able to reproduce the SARS-CoV-2 inhibition promoted by the natural neuropeptides. The inhibition profile of SARS-CoV-2 by VIP and PACAP in Calu-3 cells may be biased regarding the expected action in the lungs, since Calu-3 cells appear to express only VPAC1 [34]. However, lung tissues, while reported to express high levels of VPAC1, also express VPAC2 and PAC1 [35,37], and, more specifically, VPAC2 mRNA was detected in airway epithelial, glandular, and immune cells of the lung [36]. Therefore, while the inhibition curve of SARS-CoV-2 by VIP and PACAP in Calu-3 cells points to different optimal doses than those obtained for monocytes, it is possible that in normal lung cells and tissue, VIP and PACAP could present a broader range of action in the inhibition of SARS-CoV-2. In fact, VIP and specific agonists for VPAC1 or VPAC2 have been proposed and tested for respiratory conditions, like asthma [74–76], pulmonary arterial hypertension (PAH) [74,77,78] and chronic obstructive pulmonary disease (COPD) [74,75,79], demonstrating that the anti-inflammatory actions of VIP/PACAP can be achieved in lung tissues. Future studies should define which of these receptors would preferentially be activated by specific agonists to restrain SARS-CoV-2 replication in lungs or other sites. Together with the possible differences of receptor expression and self-regulatory characteristics of GPCRs, a third regulation level of VIP and PACAP action on pulmonary cells can be achieved by the activity of proteases and peptidases, as lungs are described to express high levels of several of them in both normal and pathological conditions [38–40]. Some of these peptidases could target VIP and PACAP, thus altering the ligand/receptor ratio and modulating the signaling pathways.

The improvement of VIP and PACAP action on SARS-CoV-2 inhibition in Calu-3 cells when combined with Bestatin, suggests that some aminopeptidases are involved in the processing or degradation of these neuropeptides. Likewise, the finding that the anti-SARS-CoV-2 effect of both neuropeptides is enhanced when they were combined with RTV, which *per se* did not inhibit SARS-CoV-2 replication but can inhibit cellular peptidases [43], supports the view that a possible clinical use of VIP or PACAP for COVID-19 treatment would be aided by a concomitant inhibition of aminopeptidases. In fact, Bestatin (Ubenimex) has already been evaluated for clinical use for some types of cancer and cardiovascular diseases, with no significant side effects [80,81]. The strong inhibition of virus production resulting from the combination of VIP and PACAP with remdesivir raises the possibility that the direct inhibition of SARS-CoV-2 transcription by this antiviral could alleviate the excessive metabolic burden on cellular processes, due to sheer reduction of viral load in the infected cells, ultimately favoring the antiviral and anti-inflammatory actions of VIP and PACAP on these cells.

Since up to now there are no antivirals specific to SARS-CoV-2, and that the hyper-inflammation may persist even after the lowering of the viral load, the searching for compounds that target the aberrant production of proinflammatory cytokines and, simultaneously, the own viral replication, should be stimulated. Our present results showing that VIP and PACAP hold these two critical activities point these neuropeptides or their analogue molecules as potential therapeutic agents for COVID-19.

Materials and Methods

Cells, virus and reagents. African green monkey kidney cells (Vero, subtype E6) and human lung epithelial cell lines (Calu-3) were expanded in high glucose DMEM (Vero) or MEM (Calu-3) with 10% fetal bovine serum (FBS; HyClone), with 100 U/mL penicillin and 100 µg/mL streptomycin (Pen/Strep; Gibco) at 37°C in a humidified atmosphere with 5% CO_2.

Peripheral blood mononuclear cells (PBMCs) were isolated by density gradient centrifugation (Ficoll-Paque, GE Healthcare) from buffy-coat preparations of blood from healthy donors. PBMCs (2 x 10^6 cells) were plated onto 48-well plates (NalgeNunc) in RPMI-1640 with 5% inactivated male human AB serum (Merck) for 3 hours. Non-adherent cells were removed and the remaining monocytes were maintained in DMEM (low-glucose) with 5% human serum (Merck) and 100 U/mL penicillin and 100 µg/mL streptomycin (Pen/Strep; Gibco). The purity of human monocytes was above 90%, as determined by flow cytometric analysis (FACScan; Becton Dickinson) using anti-CD3 (BD Biosciences) and anti-CD14 (BD Biosciences) monoclonal antibodies.

SARS-CoV-2 was expanded in Vero E6 cells from an isolate contained on a nasopharyngeal swab obtained from a confirmed case in Rio de Janeiro, Brazil (GenBank accession no. MT710714). Viral isolation was performed after a single passage in a cell culture in a 150 cm^2 flasks with high glucose DMEM plus 2% FBS. Observations for cytopathic effects were performed daily and peaked 4 to 5 days after infection. All procedures related to virus culture were handled in biosafety level 3 (BSL3) multiuser facilities according to WHO guidelines. Virus

435 titers were determined as plaque forming units (PFU/mL), and virus stocks were
436 kept in -80°C ultralow freezers.

437 The neuropeptides VIP and PACAP and the VPAC1 and VPAC2 agonists
438 (Ala^{11,22,28})-VIP and Bay 55-9837, respectively, were purchased from Tocris. The
439 PAC1 agonist Maxadilan was kindly donated by Dr. Ethan A. Lerner (Department
440 of Dermatology, Massachusetts General Hospital, MA, USA). All peptides and
441 agonists were diluted in PBS. The antivirals atazanavir (ATV), ritonavir (RTV) and
442 remdesivir (RDV) were purchased from Selleckhem, dissolved in 100%
443 dimethylsulfoxide (DMSO) and subsequently diluted at least 10^4-fold in culture or
444 reaction medium before each assay. The final DMSO concentrations showed no
445 cytotoxicity.

446 **Infections and virus titration.** Infections were performed with SARS-CoV-2 at
447 MOI of 0.01 (monocytes) or 0.1 (Calu-3) in low (monocytes) or high (Calu-3)
448 glucose DMEM without serum. After 1 hour, cells were washed and incubated with
449 complete medium with treatments or not. For virus titration, monolayers of Vero E6
450 cells (2 x 10^4 cell/well) in 96-well plates were infected with serial dilutions of
451 supernatants containing SARS-CoV-2 for 1 hour at 37°C. Semi-solid high glucose
452 DMEM medium containing 2% FSB and 2.4% carboxymethylcellulose was added
453 and cultures were incubated for 3 days at 37 °C. Then, the cells were fixed with
454 10% formalin for 2 hour at room temperature. The cell monolayer was stained with
455 0.04% solution of crystal violet in 20% ethanol for 1 hour. Plaque numbers were
456 scored in at least 3 replicates per dilution by independent readers blinded to the
457 experimental group and the virus titers were determined by plaque-forming units
458 (PFU) per milliliter.

Molecular detection of virus RNA levels. The total RNA was extracted from cultures using QIAamp Viral RNA (Qiagen®), according to manufacturer's instructions. Quantitative RT-PCR was performed using QuantiTect Probe RT-PCR Kit (Quiagen®) in a StepOnePlus™ Real-Time PCR System (Thermo Fisher Scientific). Amplifications were carried out in 15 µL reaction mixtures containing 2× reaction mix buffer, 50 µM of each primer, 10 µM of probe, and 5 µL of RNA template. Primers, probes, and cycling conditions recommended by the Centers for Disease Control and Prevention (CDC) protocol were used to detect the SARS-CoV-2 [82]. The standard curve method was employed for virus quantification. For reference to the cell amounts used, the housekeeping gene RNAse P was amplified. The Ct values for this target were compared to those obtained to different cell amounts, 10^7 to 10^2, for calibration.

SDS-PAGE and Western blot for SREBPs. After 24h of SARS-CoV-2 infection, monocytes were harvested using ice-cold lysis buffer (1% Triton X-100, 2% SDS, 150 mM NaCl, 10 mM HEPES, 2 mM EDTA containing protease inhibitor cocktail - Roche). Cell lysates were heated at 100 °C for 5 min in the presence of Laemmli buffer (20% β-mercaptoethanol; 370 mM Tris base; 160 µM bromophenol blue; 6% glycerol; 16% SDS; pH 6.8), and 20 µg of protein/sample were resolved by electrophoresis on SDS-containing 10% polyacrylamide gel (SDS-PAGE). After electrophoresis, the separated proteins were transferred to nitrocellulose membranes and incubated in blocking buffer (5% nonfat milk, 50 mM Tris-HCl, 150 mM NaCl, and 0.1% Tween 20). Membranes were probed overnight with the following antibodies: anti-SREBP-1 (Proteintech #14088-1-AP), anti-SREBP-2 (Proteintech #28212-1-AP) and anti-β-actin (Sigma, #A1978). After the washing steps, they were incubated with IRDye - LICOR or HRP-conjugated secondary

antibodies. All antibodies were diluted in blocking buffer. The detections were performed by Supersignal Chemiluminescence (GE Healthcare) or by fluorescence imaging using the Odyssey system. The densitometries were analyzed using the Image Studio Lite Ver 5.2 software.

Measurements of inflammatory mediators, cell death, NF-kBp65, CREB and neuropeptides. The levels of IL-6, IL-8, TNF-α and MIF were quantified in the supernatants from uninfected and SARS-CoV-2-infected Calu-3 cells and monocytes by ELISA (R&D Systems), following manufacturer's instructions, and results are expressed as percentages relative to uninfected cells. Cell death was determined according to the activity of lactate dehydrogenase (LDH) in the culture supernatants using a CytoTox® Kit (Promega, USA) according to the manufacturer's instructions. Results are expressed as percentages of released LDH compared to control cells lysed with 0.8% Triton X-100. Supernatants were centrifuged at 5,000 rpm for 1 minute, to remove cellular debris. Evaluation of NF-kBp65 and CREB activation was performed in infected or uninfected monocytes using NFkB p65 (Total/Phospho) InstantOne™ and CREB (Total/Phospho) Multispecies InstantOne™ ELISA Kits (Thermo Fisher), according to manufacturer's instructions. VIP and PACAP levels were quantified in the plasma from patients or control volunteers using standard commercially available ELISA and EIA Kits, according to the manufacturer's instructions (Abelisa).

Human subjects. We prospectively enrolled severe or mild/asymptomatic COVID-19 RT-PCR-confirmed cases, and SARS-CoV-2-negative controls. Blood and respiratory samples were obtained from the 24 patients with severe COVID-19 within 72 hours from intensive care unit (ICU) admission in two reference centers

(Instituto Estadual do Cérebro Paulo Niemeyer and Hospital Copa Star, Rio de Janeiro, Brazil). Severe COVID-19 was defined as those critically ill patients presenting viral pneumonia on computed tomography scan and requiring oxygen supplementation through either a nonrebreather mask or mechanical ventilation. Four outpatients presenting mild self-limiting COVID-19 syndrome, and two SARS-CoV-2-positive asymptomatic subjects were also included. All patients had SARS-CoV-2 confirmed diagnostic through RT-PCR of nasal swab or tracheal aspirates. Peripheral vein blood was also collected from 10 SARS-CoV-2-negative healthy participants as tested by RT-PCR on the day of blood sampling. The characteristics of severe (n=24), mild/asymptomatic (n=6) and healthy (n=10) participants are presented in **Table 1**. Mild and severe COVID-19 patients presented differences regarding the age and the presence of comorbidities as obesity, cardiovascular diseases and diabetes (**Table 1**), which is consistent with previously reported patient cohorts [2,83–85]. The SARS-CoV-2-negative control group, however, included subjects of older age and chronic non-communicable diseases, so it is matched with mild and critical COVID-19 patients, except for hypertension (**Table 1**). All ICU-admitted patients received usual supportive care for severe COVID-19 and respiratory support with either noninvasive oxygen supplementation (n=5) or mechanical ventilation (n=19) (**Supplemental Table 1**). Patients with acute respiratory distress syndrome (ARDS) were managed with neuromuscular blockade and a protective ventilation strategy that included low tidal volume (6 mL/kg of predicted body weight) and limited driving pressure (less than 16 cmH2O) as well as optimal PEEP calculated based on the best lung compliance and PaO2/FiO2 ratio. In those with severe ARDS and PaO2/FiO2 ratio below 150 despite optimal ventilatory settings, prone position was initiated. Our

533 management protocol included antithrombotic prophylaxis with enoxaparin 40 to
534 60 mg per day. Patients did not receive routine steroids, antivirals or other anti-
535 inflammatory or anti-platelet drugs. The SARS-CoV-2-negative control participants
536 were not under anti-inflammatory or anti-platelet drugs for at least two weeks. All
537 clinical information was prospectively collected using a standardized form -
538 ISARIC/WHO Clinical Characterization Protocol for Severe Emerging Infections
539 (CCPBR). Clinical and laboratory data were recorded on admission in all severe
540 patients included in the study and the primary outcome analyzed was 28-day
541 mortality (n = 11 survivors and 13 non-survivors, **Supplemental Table 2**). Age and
542 the frequency of comorbidities were not different between severe patients
543 requiring mechanical ventilation or noninvasive oxygen supplementation neither
544 between survivors and non-survivors (**Supplemental Table 1 and 2**).

545 **Statistical analysis.** Statistics were performed using GraphPad Prism software
546 version 8. All the numerical variables were tested regarding their distribution using
547 the Shapiro-Wilk test. One-way analysis of variance (ANOVA) was used to
548 compare differences among 3 groups following a normal (parametric) distribution,
549 and Tukey's post-hoc test was used to locate the differences between the groups;
550 or Friedman's test (for non-parametric data) with Dunn's post-hoc test.
551 Comparisons between 2 groups were performed using the Student t test for
552 parametric distributions or the Mann-Whitney U test for nonparametric
553 distributions. Correlation coefficients were calculated using Pearson's correlation
554 test for parametric distributions and the Spearman's correlation test for
555 nonparametric distributions.

Study approval. Experimental procedures involving human cells from healthy donors were performed with samples obtained after written informed consent and were approved by the Institutional Review Board (IRB) of the Oswaldo Cruz Institute/Fiocruz (Rio de Janeiro, RJ, Brazil) under the number 397-07. The National Review Board approved the study protocol (CONEP 30650420.4.1001.0008) for clinical samples, and informed consent was obtained from all participants or patients' representatives.

Acknowledgments and funding

We thank the Hemotherapy Service from Hospital Clementino Fraga Filho (Federal University of Rio de Janeiro, Brazil) for providing buffy-coats. Dr. Andre Sampaio from Farmanguinhos, platform RPT11M, and Dr. Lucio Mendes Cabral from Department of Drugs and Pharmaceutics, Faculty of Pharmacy, Federal University of Rio de Janeiro (UFRJ) are acknowledged for kindly donating the Calu-3 cell. The recombinant protein Maxadilan was kindly donated to us by Dr. Ethan A. Lerner (Department of Dermatology, Massachusetts General Hospital, MA, USA). The authors are thankful to Prof. Elvira M. Saraiva (Federal University of Rio de Janeiro, Brazil) for stimulating comments and invaluable suggestions. This work was supported by Conselho Nacional de Desenvolvimento Científico e Tecnológico (CNPq), Fundação de Amparo à Pesquisa do Estado do Rio de Janeiro (FAPERJ), and by Mercosur Structural Convergence Fund (FOCEM, Mercosur, grant number 03/11). This study was financed in part by the Coordenação de Aperfeiçoamento de Pessoal de Nível Superior - Brasil (CAPES), Finance Code 001. Funding was also provided by CNPq, CAPES and FAPERJ through the National Institutes of Science and Technology Program (INCT) to

Carlos Morel (INCT-IDPN) and Wilson Savino (INCT-NIM). Thanks are due to Oswaldo Cruz Foundation/Fiocruz under the auspicious of Inova program. The funding sponsors had no role in the design of the study; in the collection, analyses, or interpretation of data; in the writing of the manuscript, and in the decision to publish the results. The authors declare no competing financial interests.

Author Contribution

Conceived the study: JRT, TMLS, DCBH; Designed the experiments: JRT, PTB, TMLS, DCBH; Performed the experiments: JRT, CQS, NFR, CRRP, CSF, SSGD, ACF, MM, VCS, LT, IGAQ, EDH, PK; Analyzed the data: JRT, PTB, IGAQ, EDH, PK, FAB, TMLS, DCBH; Wrote the paper: JRT, PTB, TMLS, DCBH. All authors reviewed and approved the manuscript.

References

1. García, L. F. Immune Response, Inflammation, and the Clinical Spectrum of COVID-19. *Front. Immunol.* **11**, (2020).

2. Huang, C. *et al.* Clinical features of patients infected with 2019 novel coronavirus in Wuhan, China. *Lancet* **395**, 497–506 (2020).

3. Chen, G. *et al.* Clinical and immunological features of severe and moderate coronavirus disease 2019. *J. Clin. Invest.* **130**, 2620–2629 (2020).

4. Gupta, A. *et al.* Extrapulmonary manifestations of COVID-19. *Nat. Med.* **26**, 1017–1032 (2020).

5. Tang, D., Comish, P. & Kang, R. The hallmarks of COVID-19 disease. *PLoS Pathogens* vol. 16 e1008536 (2020).

6. Ragab, D., Salah Eldin, H., Taeimah, M., Khattab, R. & Salem, R. The COVID-19 Cytokine Storm; What We Know So Far. *Front. Immunol.* **11**, (2020).

7. Giamarellos-Bourboulis, E. J. *et al.* Complex Immune Dysregulation in COVID-19 Patients with Severe Respiratory Failure. *Cell Host Microbe* **27**, 992-1000.e3 (2020).

8. Blanco-Melo, D. *et al.* Imbalanced Host Response to SARS-CoV-2 Drives Development of COVID-19. *Cell* **181**, 1036-1045.e9 (2020).

9. Veras, F. P. *et al.* SARS-CoV-2-triggered neutrophil extracellular traps mediate COVID-19

pathology. *J. Exp. Med.* **217**, (2020).

10. Radermecker, C. *et al.* Neutrophil extracellular traps infiltrate the lung airway, interstitial, and vascular compartments in severe COVID-19. *J. Exp. Med.* **217**, (2020).

11. Skendros, P. *et al.* Complement and tissue factor–enriched neutrophil extracellular traps are key drivers in COVID-19 immunothrombosis. *J. Clin. Invest.* **130**, 6151–6157 (2020).

12. Middleton, E. A. *et al.* Neutrophil extracellular traps contribute to immunothrombosis in COVID-19 acute respiratory distress syndrome. *Blood* **136**, 1169–1179 (2020).

13. Rodrigues, T. S. *et al.* Inflammasomes are activated in response to SARS-CoV-2 infection and are associated with COVID-19 severity in patients. *J. Exp. Med.* **218**, (2021).

14. Ferreira, A. C. *et al.* SARS-CoV-2 induces inflammasome-dependent pyroptosis and downmodulation of HLA-DR in human monocytes. *medRxiv* 2020.08.25.20182055 (2020) doi:10.1101/2020.08.25.20182055.

15. Nicholls, J. M. *et al.* Lung pathology of fatal severe acute respiratory syndrome. *Lancet* **361**, 1773–1778 (2003).

16. Gu, J. *et al.* Multiple organ infection and the pathogenesis of SARS. *J. Exp. Med.* **202**, 415–424 (2005).

17. Merad, M. & Martin, J. C. Pathological inflammation in patients with COVID-19: a key role for monocytes and macrophages. *Nat. Rev. Immunol.* **20**, 355–362 (2020).

18. Schurink, B. *et al.* Viral presence and immunopathology in patients with lethal COVID-19: a prospective autopsy cohort study. *The Lancet Microbe* **1**, e290–e299 (2020).

19. Chiang, C.-C., Korinek, M., Cheng, W.-J. & Hwang, T.-L. Targeting Neutrophils to Treat Acute Respiratory Distress Syndrome in Coronavirus Disease. *Front. Pharmacol.* **11**, 1576 (2020).

20. Zhou, J. *et al.* Active replication of middle east respiratory syndrome coronavirus and aberrant induction of inflammatory cytokines and chemokines in human macrophages: Implications for pathogenesis. *J. Infect. Dis.* **209**, 1331–1342 (2014).

21. Tynell, J. *et al.* Middle east respiratory syndrome coronavirus shows poor replication but significant induction of antiviral responses in human monocyte-derived macrophages and dendritic cells. *J. Gen. Virol.* **97**, 344–355 (2016).

22. Dickson, L. & Finlayson, K. VPAC and PAC receptors: From ligands to function. *Pharmacol Ther* **121**, 294–316 (2009).

23. Ganea, D. & Delgado, M. Vasoactive intestinal peptide (VIP) and pituitary adenylate cyclase-activating polypeptide (PACAP) as modulators of both innate and adaptive immunity. *Crit Rev Oral Biol Med* **13**, 229–237 (2002).

24. Kim, W. K. *et al.* Vasoactive intestinal peptide and pituitary adenylyl cyclase-activating polypeptide inhibit tumor necrosis factor-α production in injured spinal cord and in activated microglia via a cAMP-dependent pathway. *J. Neurosci.* **20**, 3622–3630 (2000).

25. Larocca, L., Calafat, M., Roca, V., Franchi, A. M. & Leiros, C. P. VIP limits LPS-induced nitric oxide production through IL-10 in NOD mice. *Int Immunopharmacol* **7**, 1343–1349 (2007).

26. Gonzalez-Rey, E. & Delgado, M. Vasoactive intestinal peptide inhibits cycloxygenase-2 expression in activated macrophages, microglia, and dendritic cells. *Brain. Behav. Immun.* **22**, 35–41 (2008).

27. Delgado, M., Munoz-Elias, E. J., Gomariz, R. P. & Ganea, D. VIP and PACAP inhibit IL-12 production in LPS-stimulated macrophages. Subsequent effect on IFNγ synthesis by T cells. *J. Neuroimmunol.* **96**, 167–181 (1999).

28. Delgado, M., Munoz-Elias, E. J., Gomariz, R. P. & Ganea, D. Vasoactive intestinal peptide and pituitary adenylate cyclase-activating polypeptide prevent inducible nitric oxide synthase transcription in macrophages by inhibiting NF-kappa B and IFN regulatory factor 1 activation. *J. Immunol.* **162**, 4685–96 (1999).

29. Moody, T. W., Ito, T., Osefo, N. & Jensen, R. T. VIP and PACAP: recent insights into their functions/roles in physiology and disease from molecular and genetic studies. *Curr Opin Endocrinol Diabetes Obes* **18**, 61–67 (2011).

30. Gonzalez-Rey, E., Varela, N., Chorny, A. & Delgado, M. Therapeutical Approaches of Vasoactive Intestinal Peptide as a Pleiotropic Immunomodulator. *Curr. Pharm. Des.* **13**, 1113–1139 (2007).

31. Pozo, D. *et al.* Tuning immune tolerance with vasoactive intestinal peptide: A new therapeutic approach for immune disorders. *Peptides* **28**, 1833–1846 (2007).

32. Temerozo, J. R. J. R., Joaquim, R., Regis, E. G. E. G., Savino, W. & Bou-Habib, D. C. D. C. D. C. Macrophage Resistance to HIV-1 Infection Is Enhanced by the Neuropeptides VIP and PACAP. *PLoS One* **8**, (2013).

33. Temerozo, J. R. J. R. *et al.* The Neuropeptides Vasoactive Intestinal Peptide and Pituitary Adenylate Cyclase-Activating Polypeptide Control HIV-1 Infection in Macrophages Through Activation of Protein Kinases A and C. *Front. Immunol.* **9**, (2018).

34. Dérand, R. *et al.* Activation of VPAC 1 receptors by VIP and PACAP-27 in human bronchial epithelial cells induces CFTR-dependent chloride secretion. *Br. J. Pharmacol.* **141**, 698–708 (2004).

35. Busto, R., Prieto, J. C., Bodega, G., Zapatero, J. & Carrero, I. Immunohistochemical localization and distribution of VIP/PACAP receptors in human lung. *Peptides* **21**, 265–269 (2000).

36. Groneberg, D. A., Hartmann, P., Dinh, Q. T. & Fischer, A. Expression and distribution of vasoactive intestinal polypeptide receptor VPAC2 mRNA in human airways. *Lab. Investig.* **81**, 749–755 (2001).

37. Fagerberg, L. *et al.* Analysis of the human tissue-specific expression by genome-wide integration of transcriptomics and antibody-based proteomics. *Mol. Cell. Proteomics* **13**, 397–406 (2014).

38. Van Der Velden, V. H. J. *et al.* Expression of aminopeptidase N and dipeptidyl peptidase IV in the healthy and asthmatic bronchus. *Clin. Exp. Allergy* **28**, 110–120 (1998).

39. Dreymueller, D., Uhlig, S. & Ludwig, A. ADAM-family metalloproteinases in lung inflammation: potential therapeutic targets. *Am. J. Physiol. Cell. Mol. Physiol.* **308**, L325–L343 (2015).

689 40. Bonda, W. L. M., Iochmann, S., Magnen, M., Courty, Y. & Reverdiau, P. Kallikrein-related
690 peptidases in lung diseases. *Biol. Chem.* **399**, 959–971 (2018).

691 41. Kolb, A. F. *et al.* Molecular analysis of the coronavirus-receptor function of aminopeptidase
692 N. *Adv. Exp. Med. Biol.* **440**, 61–7 (1998).

693 42. Ou, X. *et al.* Characterization of spike glycoprotein of SARS-CoV-2 on virus entry and its
694 immune cross-reactivity with SARS-CoV. *Nat. Commun.* **11**, 1620 (2020).

695 43. Kourjian, G. *et al.* Sequence-Specific Alterations of Epitope Production by HIV Protease
696 Inhibitors. *J. Immunol.* **192**, 3496–3506 (2014).

697 44. Fintelman-Rodrigues, N. *et al.* Atazanavir, alone or in combination with ritonavir, inhibits
698 SARS-CoV-2 replication and proinflammatory cytokine production. *Antimicrob. Agents*
699 *Chemother.* **64**, (2020).

700 45. Pruijssers, A. J. *et al.* Remdesivir Inhibits SARS-CoV-2 in Human Lung Cells and Chimeric
701 SARS-CoV Expressing the SARS-CoV-2 RNA Polymerase in Mice. *Cell Rep.* **32**, 107940
702 (2020).

703 46. Delgado, M., Garrido, E., Martinez, C., Leceta, J. & Gomariz, R. P. Vasoactive intestinal
704 peptide and pituitary adenylate cyclase-activating polypeptides (PACAP27) and PACAP38)
705 protect CD4+CD8+ thymocytes from glucocorticoid-induced apoptosis. *Blood* **87**, 5152–
706 5161 (1996).

707 47. Liu, T., Zhang, L., Joo, D. & Sun, S.-C. NF-κB signaling in inflammation. *Signal Transduct.*
708 *Target. Ther.* **2**, 17023 (2017).

709 48. Schomerus, C., Maronde, E., Laedtke, E. & Korf, H. W. Vasoactive intestinal peptide (VIP)
710 and pituitary adenylate cyclase-activating polypeptide (PACAP) induce phosphorylation of
711 the transcription factor CREB in subpopulations of rat pinealocytes: immunocytochemical
712 and immunochemical evidence. *Cell Tissue Res* **286**, 305–313 (1996).

713 49. Matt, T. Transcriptional control of the inflammatory response: a role for the CREB-binding
714 protein (CBP). *Acta Med Austriaca* **29**, 77–79 (2002).

715 50. Wen, A. Y., Sakamoto, K. M. & Miller, L. S. The Role of the Transcription Factor CREB in
716 Immune Function. *J. Immunol.* **185**, 6413–6419 (2010).

717 51. Shenkar, R., Yum, H.-K., Arcaroli, J., Kupfner, J. & Abraham, E. Interactions between CBP,
718 NF-κB, and CREB in the lungs after hemorrhage and endotoxemia. *Am. J. Physiol. Cell. Mol.*
719 *Physiol.* **281**, L418–L426 (2001).

720 52. Toth, J. I., Datta, S., Athanikar, J. N., Freedman, L. P. & Osborne, T. F. Selective Coactivator
721 Interactions in Gene Activation by SREBP-1a and -1c. *Mol. Cell. Biol.* **24**, 8288–8300 (2004).

722 53. Yuan, S. *et al.* SREBP-dependent lipidomic reprogramming as a broad-spectrum antiviral
723 target. *Nat. Commun.* **10**, 120 (2019).

724 54. Cloherty, A. P. M., Olmstead, A. D., Ribeiro, C. M. S. & Jean, F. Hijacking of Lipid Droplets by
725 Hepatitis C, Dengue and Zika Viruses—From Viral Protein Moonlighting to Extracellular
726 Release. *Int. J. Mol. Sci.* **21**, 7901 (2020).

727 55. Taylor, H. E., Linde, M. E., Khatua, A. K., Popik, W. & Hildreth, J. E. K. Sterol Regulatory
728 Element-Binding Protein 2 Couples HIV-1 Transcription to Cholesterol Homeostasis and T

729 Cell Activation. *J. Virol.* **85**, 7699–7709 (2011).

730 56. Dias, S. da S. G. *et al.* Lipid droplets fuel SARS-CoV-2 replication and production of
731 inflammatory mediators. *PLOS Pathog.* **16**, e1009127 (2020).

732 57. Lee, W. *et al.* COVID-19-activated SREBP2 disturbs cholesterol biosynthesis and leads to
733 cytokine storm. *Signal Transduct. Target. Ther.* **5**, (2020).

734 58. NCT0431169. Intravenous Aviptadil for Critical COVID-19 With Respiratory Failure.
735 *[ClinicalTrials.gov] Bethesda (MD): National Library of Medicine (US).*
736 https://clinicaltrials.gov/ct2/show/NCT04311697.

737 59. NCT04536350. Inhaled Aviptadil for the Treatment of Moderate and Severe COVID-19.
738 *[ClinicalTrials.gov] Bethesda (MD): National Library of Medicine (US).*
739 https://clinicaltrials.gov/ct2/show/NCT04360096.

740 60. Said, S. I. The discovery of VIP: Initially looked for in the lung, isolated from intestine, and
741 identified as a neuropeptide. *Peptides* **28**, 1620–1621 (2007).

742 61. Delgado, M., Munoz-Elias, E. J., Martinez, C., Gomariz, R. P. & Ganea, D. VIP and PACAP38
743 modulate cytokine and nitric oxide production in peritoneal. *Ann N Y Acad Sci* **897**, 401–
744 414 (1999).

745 62. Parry, G. C. & Mackman, N. Role of cyclic AMP response element-binding protein in cyclic
746 AMP inhibition of NF-kappaB-mediated transcription. *J. Immunol.* **159**, 5450–6 (1997).

747 63. Ollivier, V., Parry, G. C. N., Cobb, R. R., de Prost, D. & Mackman, N. Elevated Cyclic AMP
748 Inhibits NF-κB-mediated Transcription in Human Monocytic Cells and Endothelial Cells. *J.*
749 *Biol. Chem.* **271**, 20828–20835 (1996).

750 64. Luan, B. *et al.* CREB pathway links PGE2 signaling with macrophage polarization. *Proc. Natl.*
751 *Acad. Sci. U. S. A.* **112**, 15642–15647 (2015).

752 65. Zhao, L. Suppression of Proinflammatory Cytokines Interleukin-1 and Tumor Necrosis
753 Factor- in Astrocytes by a V1 Vasopressin Receptor Agonist: A cAMP Response Element-
754 Binding Protein-Dependent Mechanism. *J. Neurosci.* **24**, 2226–2235 (2004).

755 66. Morris, R. H. K. *et al.* DPPC regulates COX-2 expression in monocytes via phosphorylation
756 of CREB. *Biochem. Biophys. Res. Commun.* **370**, 174–178 (2008).

757 67. Ernst, O. *et al.* Exclusive Temporal Stimulation of IL-10 Expression in LPS-Stimulated Mouse
758 Macrophages by cAMP Inducers and Type I Interferons. *Front. Immunol.* **10**, 1788 (2019).

759 68. Barátki, B. L., Huber, K., Sármay, G., Matkó, J. & Kövesdi, D. Inflammatory signal induced IL-
760 10 production of marginal zone B-cells depends on CREB. *Immunol. Lett.* **212**, 14–21
761 (2019).

762 69. Avni, D., Ernst, O., Philosoph, A. & Zor, T. Role of CREB in modulation of TNFα and IL-10
763 expression in LPS-stimulated RAW264.7 macrophages. *Mol. Immunol.* **47**, 1396–1403
764 (2010).

765 70. Park, J. M. *et al.* Signaling Pathways and Genes that Inhibit Pathogen-Induced Macrophage
766 Apoptosis— CREB and NF-κB as Key Regulators. *Immunity* **23**, 319–329 (2005).

767 71. Cheng, J. C. *et al.* CREB is a critical regulator of normal hematopoiesis and leukemogenesis.
768 *Blood* **111**, 1182–1192 (2008).

72. Shimano, H. & Sato, R. SREBP-regulated lipid metabolism: convergent physiology — divergent pathophysiology. *Nat. Rev. Endocrinol.* **13**, 710–730 (2017).

73. Harikumar, K. G., Morfis, M. M., Lisenbee, C. S., Sexton, P. M. & Miller, L. J. Constitutive formation of oligomeric complexes between family B G protein-coupled vasoactive intestinal polypeptide and secretin receptors. *Mol Pharmacol* **69**, 363–373 (2006).

74. Wu, D., Lee, D. & Sung, Y. K. Prospect of vasoactive intestinal peptide therapy for COPD/PAH and asthma: a review. *Respir. Res.* **12**, 45 (2011).

75. Onoue, S., Yamada, S. & Yajima, T. Bioactive analogues and drug delivery systems of vasoactive intestinal peptide (VIP) for the treatment of asthma/COPD. *Peptides* **28**, 1640–1650 (2007).

76. Lindén, A. *et al.* Bronchodilation by an inhaled VPAC2 receptor agonist in patients with stable asthma. *Thorax* **58**, 217–221 (2003).

77. Hamidi, S. A. *et al.* VIP and endothelin receptor antagonist: An effective combination against experimental pulmonary arterial hypertension. *Respir. Res.* **12**, (2011).

78. Hilaire, R. C., Murthya, S. N., Kadowitza, P. J. & Jeter, J. R. Role of VPAC1 and VPAC2 in VIP mediated inhibition of rat pulmonary artery and aortic smooth muscle cell proliferation. *Peptides* **31**, 1517–1522 (2010).

79. Burian, B., Angela, S., Nadler, B., Petkov, V. & Block, L. H. Inhaled Vasoactive Intestinal Peptide (VIP) improves the 6-minute walk test and quality of life in patients with COPD: The VIP/COPD-trial. *Chest* **130**, 121S (2006).

80. Wakita, A. *et al.* Randomized comparison of fixed-schedule versus response-oriented individualized induction therapy and use of ubenimex during and after consolidation therapy for elderly patients with acute myeloid leukemia: the JALSG GML200 Study. *Int. J. Hematol.* **96**, 84–93 (2012).

81. Ichinose, Y. *et al.* Randomized double-blind placebo-controlled trial of bestatin in patients with resected stage I squamous-cell lung carcinoma. *J. Natl. Cancer Inst.* **95**, 605–10 (2003).

82. CDC. Real-time RT-PCR Primers and Probes for COVID-19. *Centers for Disease Control and Prevention* https://www.cdc.gov/coronavirus/2019-ncov/lab/rt-pcr-panel-primer-probes.html (2020).

83. Wu, C. *et al.* Risk Factors Associated With Acute Respiratory Distress Syndrome and Death in Patients With Coronavirus Disease 2019 Pneumonia in Wuhan, China. *JAMA Intern. Med.* **180**, 934 (2020).

84. Shi, S. *et al.* Association of Cardiac Injury With Mortality in Hospitalized Patients With COVID-19 in Wuhan, China. *JAMA Cardiol.* **5**, 802 (2020).

85. Guo, T. *et al.* Cardiovascular Implications of Fatal Outcomes of Patients With Coronavirus Disease 2019 (COVID-19). *JAMA Cardiol.* **5**, 811 (2020).

807 ## Figure legends

808 **Figure 1. VIP and PACAP inhibit SARS-CoV-2 gene replication in monocytes and**
809 **protect the cells from virus-mediated cytopathicity.** (A, B) Monocytes were infected
810 with SARS-CoV-2 and exposed to the indicated concentrations of (A) VIP or (B) PACAP.
811 Virus RNA synthesis was evaluated by qPCR in the culture supernatants 24 hours after
812 infection. (C) Cellular viability was analyzed by measuring LDH release in the
813 supernatants of uninfected or SARS-CoV-2-infected monocytes, treated or not with VIP or
814 PACAP. (D, E) Similar to A and B, except that cells were treated with agonists for VIP and
815 PACAP receptors, as indicated, at different concentrations (D) or with combined
816 equivalent doses VIP and PACAP (E). Data in A, B, D and E are shown normalized to
817 infected cells kept only with culture medium, and in C represent means ± SD of absolute
818 values. *$p \leq .05$; **$p \leq .01$. (A, B) n=5; (D) n=6; (D, E) n=4

819 **Figure 2**. **VIP and PACAP inhibit SARS-CoV-2 replication in Calu-3 cells, protect the**
820 **cells from virus-mediated cytopathicity, and mediate transmission of viral**
821 **resistance from monocytes to human lung cells.** Calu-3 cells were infected by SARS-
822 CoV-2 and then left untreated (0) or treated with the indicated concentrations of VIP (A) or
823 PACAP (B). After 48 hours, supernatants were collected, and viral replication was
824 evaluated by quantifying PFUs in plaque assays. (C) Cellular viability was analyzed by
825 measuring LDH release in the supernatants of uninfected or SARS-CoV-2-infected Calu-3
826 cells, treated or not with VIP (1 nM) or PACAP (50 nM). (D) Similar to A and B, except that
827 cells were treated with agonists for VIP and PACAP receptors, as indicated, at different
828 concentrations. (E, three bars on the left) SARS-CoV-2-infected Calu-3 cells were kept
829 untreated (Control) or received CM (50% final dilution) from VIP- or PACAP-treated
830 uninfected monocytes. (E, three bars on the right) SARS-CoV-2-infected Calu-3 cells were
831 kept untreated (Control) or received CM (50% final dilution) from VIP- or PACAP-treated
832 SARS-CoV-2-infected monocytes. After 48 hours, supernatants were collected, and viral

833 replication was evaluated by quantifying PFUs in plaque assay. Data are shown as means
834 ± SD. *$p \leq .05$; **$p \leq .01$. (A, B, C, D) n=4; (E) n=5

835 **Figure 3**. **Influence of peptidases on VIP- or PACAP-induced inhibition of SARS-**
836 **CoV-2 replication in pulmonary cells.** Calu-3 cells were infected with SARS-CoV-2 and
837 treated with Bestatin at 500 nM (A), or with the indicated concentrations of VIP (B) or
838 PACAP (C) associated or not with Bestatin 500 nM. After 48 hours, supernatants were
839 collected, and viral replication was evaluated by quantifying PFUs in plaque assay. Data
840 are shown as means ± SD. * and + represent $p \leq .05$ versus control (0), and # represents
841 $p \leq .05$ of neuropeptide versus neuropeptide + Bestatin at indicated concentrations. (A, B,
842 C) n=4

843 **Figure 4. Association with antivirals increments the neuropeptide anti-SARS-CoV-2**
844 **effect in pulmonary cells.** Calu-3 cells were infected with SARS-CoV-2 and treated with
845 ATV 5 uM, RTV 5 uM or RDV 0.1 uM (A), or with the indicated concentrations of VIP (B)
846 or PACAP (C) associated or not with ATV, RTV or RDV. After 48 hours, supernatants
847 were collected, and viral replication was evaluated by quantifying PFUs in plaque assay.
848 Data are shown as means ± SD. *, +, # and § represent $p \leq .05$ versus control (0), and "x"
849 represents $p \leq .05$ of neuropeptide versus neuropeptide + RTV (5 nM). (A, B, C) n=4

850 **Figure 5**. **VIP and PACAP reduce production of proinflammatory mediators by**
851 **SARS-CoV-2-infected monocytes and Calu-3 cells.** Monocytes and Calu-3 cells were
852 infected with SARS-CoV-2 for 1 hour, and then exposed to VIP or PACAP (10 nM each for
853 monocytes, 1 nM of VIP or 50 nM of PACAP for Calu-3 cells). The levels of IL-6, IL-8,
854 TNF-α and MIF were measured in culture supernatants of monocytes after 24 hours (A),
855 and of IL-6 and IL-8 after 48 hours for Calu-3 cells (B), by ELISA. Data represent means ±
856 SD. *$p \leq .05$; **$p \leq .01$. (A) n=6; (B) n=4

857 **Figure 6**. **VIP and PACAP regulate the activation of transcription factors in SARS-**
858 **CoV-2-infected monocytes.** Monocytes were infected by SARS-CoV-2 and, 1 hour later,
859 the infected cells were exposed (or not - Nil) to VIP or PACAP (at 10 nM). After 24 hours,
860 the cells were lysed and the ratios between phosphoNF-kBp65/total NF-kBp65 (A),
861 phosphoCREB/total CREB (B), active SREBP-1/β-actin (C), and active SREBP-2/β-actin
862 (D) were quantified by ELISA (A and B) or by western blot (C and D) in the cell lysates.
863 Data represent means ± SD. *$p \leq .05$; **$p \leq .01$; ***$p \leq .001$. (A, B) n=3; (C, D) n=4

864 **Figure 7**. **Plasma level of VIP is elevated in patients with severe forms of COVID-19.**
865 The levels of VIP (A) and PACAP (B) in the plasma of SARS-CoV-2-negative control
866 participants, SARS-CoV-2-positive asymptomatic subjects, or symptomatic patients
867 presenting mild to severe COVID-19 syndrome were quantified by ELISA. Correlation
868 between levels of VIP and CRP (C) and levels of both neuropeptides (D) in the plasma
869 from patients with COVID-19. Correlation between viral load and VIP (E) or PACAP (F) in
870 mild and severe patients with detectable swabs samples. (G and I) Severe COVID-19
871 patients admitted to the ICU were stratified between those requiring invasive mechanical
872 ventilation or noninvasive O_2 supplementation. (H and J) Severe COVID-19 patients were
873 stratified according to the 28-day mortality outcome as survivors or non survivors. One
874 outlier (CRP = 621.64 mg/dL) was excluded from the analysis in panels C-D according to
875 the ROUT test. Linear regression (with the 95 % confidence interval) and Spearman's
876 correlation were calculated according to the distribution of the dots (controls: grey;
877 asymptomatics: brown; mild: green; severe: red). The horizontal lines in the box plots
878 represent the median, the box edges represent the interquartile ranges, and the whiskers
879 indicate the minimal and maximal value in each group. *$p \leq .05$; **$p \leq .01$.

880

881 **Table 1:** Characteristics of COVID-19 patients and control subjects.

Characteristics[1]	Control (n=10)	Asymptomatical/ Mild (n=6)	Severe/critical (n=24)
Age, years	53 (32 – 60)	31 (29 – 34)	58 (48 – 66)
Sex, male	4 (40%)	2 (33.3 %)	12 (50 %)
Respiratory support			
Oxygen supplementation	0 (0%)	0 (0%)	5 (20.8%)
Mechanical ventilation	0 (0%)	0 (0%)	19 (79.2%)
SAPS 3	-	-	60 (55 – 71)
PaO2/FiO2 ratio	-	-	154 (99 – 373)
Vasopressor	-	-	10 (41.6%)
Time from symptom onset to blood sample, days	-	5 (-1 – 7)[2]	14 (8 – 17)
28-day mortality	-	-	13 (54.2%)
Comorbidities			
Obesity	1 (10%)	0 (0%)	5 (20.8%)
Hypertension	1 (10%)	0 (0%)	6 (25%)
Diabetes	0 (0%)	0 (0%)	9 (37.5%)
Cancer	0 (0%)	0 (0%)	3 (12.5%)
Heart disease[3]	0 (0%)	0 (0%)	2 (8.3%)
Presenting symptoms			
Cough	0 (0%)	3 (50%)	17 (70.8%)
Fever	0 (0%)	2 (33.3%)	18 (75%)
Dyspnea	0 (0%)	0 (0%)	20 (83.3%)
Headache	0 (0%)	2 (33.3%)	3 (12.5%)
Anosmia	0 (0%)	1 (16.6%)	8 (33.3%)
Laboratory findings on admission			
Leukocytes, x 1000/µL	-	-	138 (102 – 180)
Lymphocyte, cells/µL	-	-	1,167 (645 – 1,590)
Monocytes, cells/µL	-	-	679 (509 – 847)
Platelet count, x 1000/µL	-	-	169 (137 – 218)
C Reactive Protein, mg/L[4]	0.1 (0.1 – 0.18)	0.1 (0.1 – 0.11)	178 (74 – 308)*
Fibrinogen, mg/dL[4]	281 (232 – 302)	229 (197 – 324)	528 (366 – 714)*
D-dimer, IU/mL[4]	292 (225 – 476)	191 (190 – 291)	4836 (2364 – 10816)*
IL-6, pg/mL	13 (7 – 16)	9 (7.7 – 9.2)	33.5 (19.2 – 76.7)*

882 [1]Numerical variables are represented as the median and the interquartile range, and
883 qualitative variables are represented as the number and the percentage.
884 [2]Day of sample collection after the onset of symptoms was not computed for
885 asymptomatic subjects.
886 [3]Coronary artery disease or congestive heart failure.
887 [4]Reference values of C reactive Protein (0.00 – 1.00), Fibrinogen (238 – 498 mg/dL) and
888 D-dimer (0 – 500 ng/mL).
889 *$p < 0.05$ compared to control. The qualitative variables were compared using the two
890 tailed Fisher exact test, and the numerical variables using the t test for parametric and the
891 Mann Whitney U test for nonparametric distributions.

Figure 1

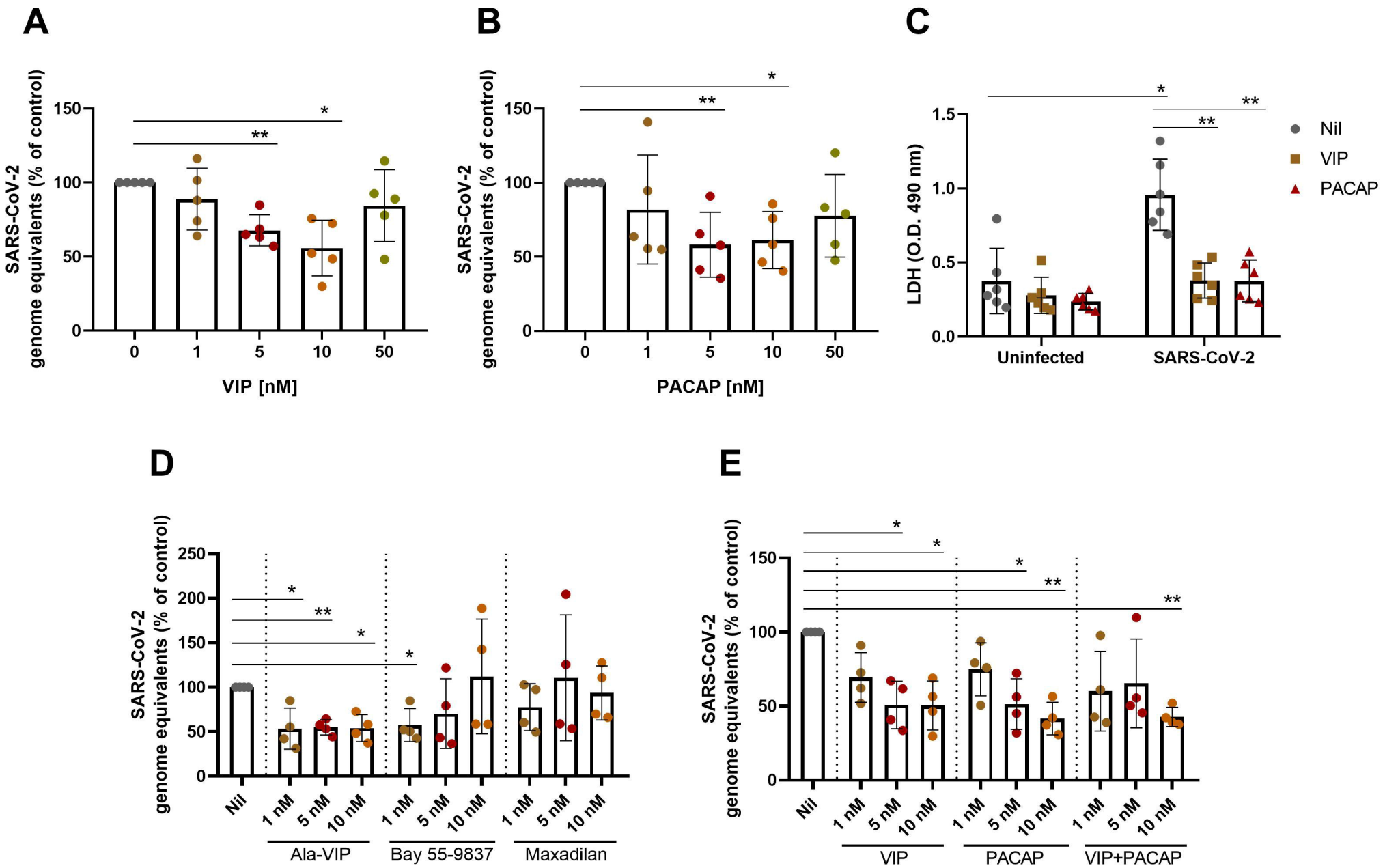
A
SARS-CoV-2 genome equivalents (% of control)
150
100
50
0
0
1
5
10
50
VIP [nM]
*
**
B
SARS-CoV-2 genome equivalents (% of control)
150
100
50
0
0
1
5
10
50
PACAP [nM]
*
**
C
LDH (O.D. 490 nm)
1.5
1.0
0.5
0.0
Uninfected
SARS-CoV-2
*
**
**
Nil
VIP
PACAP
D
SARS-CoV-2 genome equivalents (% of control)
250
200
150
100
50
0
Nil
1 nM
5 nM
10 nM
Ala-VIP
Bay 55-9837
Maxadilan
*
**
*
*
E
SARS-CoV-2 genome equivalents (% of control)
150
100
50
0
Nil
1 nM
5 nM
10 nM
VIP
PACAP
VIP+PACAP
*
*
*
**
**

Figure 2

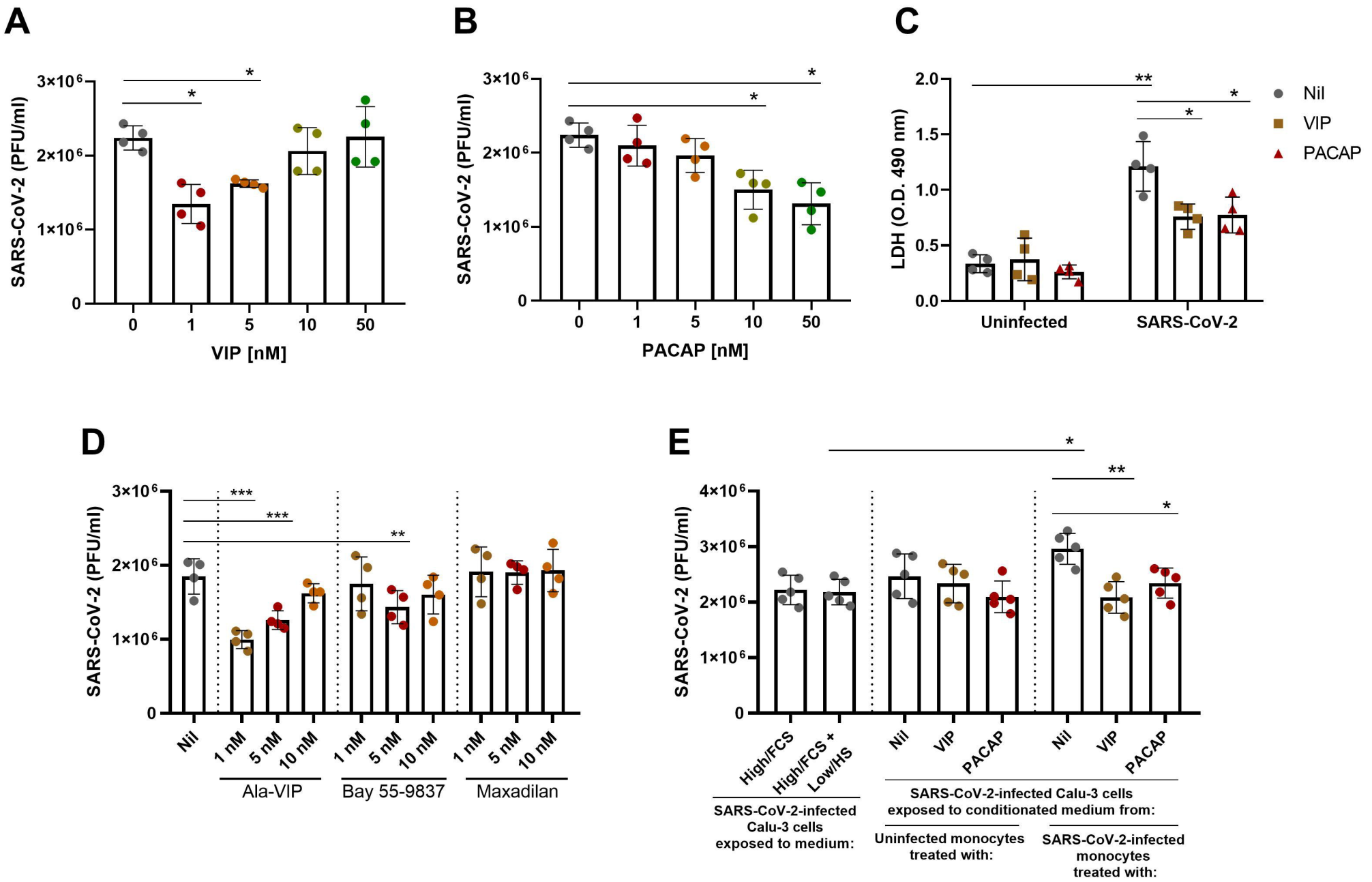
A
SARS-CoV-2 (PFU/ml)
3×10⁶
2×10⁶
1×10⁶
0
*
*
0
1
5
10
50
VIP [nM]
B
SARS-CoV-2 (PFU/ml)
3×10⁶
2×10⁶
1×10⁶
0
*
*
0
1
5
10
50
PACAP [nM]
C
LDH (O.D. 490 nm)
2.0
1.5
1.0
0.5
0.0
**
*
*
Uninfected
SARS-CoV-2
Nil
VIP
PACAP
D
SARS-CoV-2 (PFU/ml)
3×10⁶
2×10⁶
1×10⁶
0
***
***
**
Nil
1 nM
5 nM
10 nM
1 nM
5 nM
10 nM
1 nM
5 nM
10 nM
Ala-VIP
Bay 55-9837
Maxadilan
E
SARS-CoV-2 (PFU/ml)
4×10⁶
3×10⁶
2×10⁶
1×10⁶
0
*
**
*
High/FCS
High/FCS + Low/HS
Nil
VIP
PACAP
Nil
VIP
PACAP
SARS-CoV-2-infected Calu-3 cells exposed to medium:
SARS-CoV-2-infected Calu-3 cells exposed to conditionated medium from:
Uninfected monocytes treated with:
SARS-CoV-2-infected monocytes treated with:

Figure 3

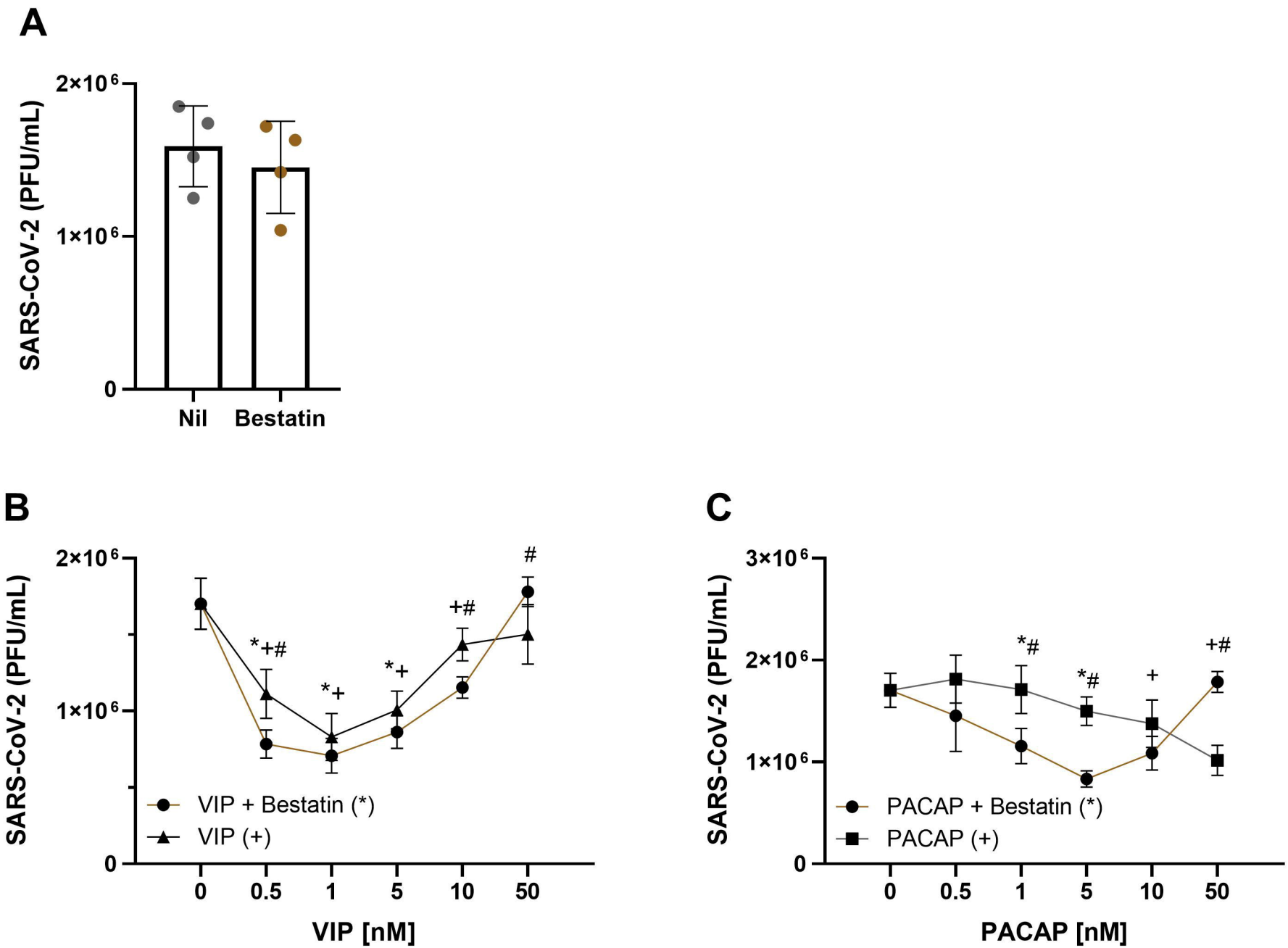
A
SARS-CoV-2 (PFU/mL)
2×10⁶
1×10⁶
0
Nil
Bestatin
B
SARS-CoV-2 (PFU/mL)
2×10⁶
1×10⁶
0
*+#
*+
*+
+#
#
VIP + Bestatin (*)
VIP (+)
0
0.5
1
5
10
50
VIP [nM]
C
SARS-CoV-2 (PFU/mL)
3×10⁶
2×10⁶
1×10⁶
0
*#
*#
+
+#
PACAP + Bestatin (*)
PACAP (+)
0
0.5
1
5
10
50
PACAP [nM]

Figure 4

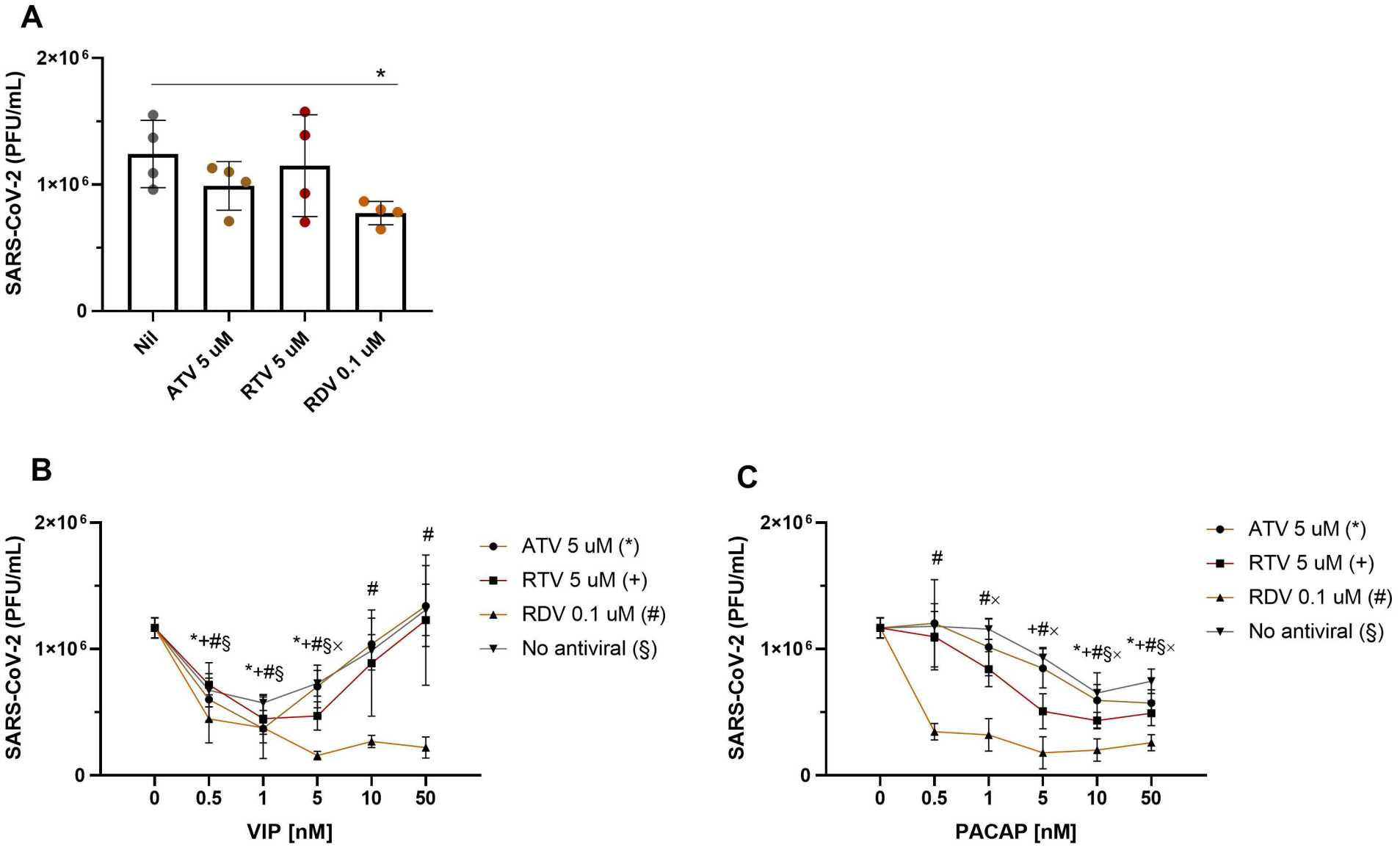
A
2×10⁶
1×10⁶
0
SARS-CoV-2 (PFU/mL)
*
Nil
ATV 5 uM
RTV 5 uM
RDV 0.1 uM
B
SARS-CoV-2 (PFU/mL)
*+#§
*+#§
*+#§×
#
#
0
0.5
1
5
10
50
VIP [nM]
ATV 5 uM (*)
RTV 5 uM (+)
RDV 0.1 uM (#)
No antiviral (§)
C
SARS-CoV-2 (PFU/mL)
#
#×
+#×
*+#§×
*+#§×
PACAP [nM]
ATV 5 uM (*)
RTV 5 uM (+)
RDV 0.1 uM (#)
No antiviral (§)

Figure 5

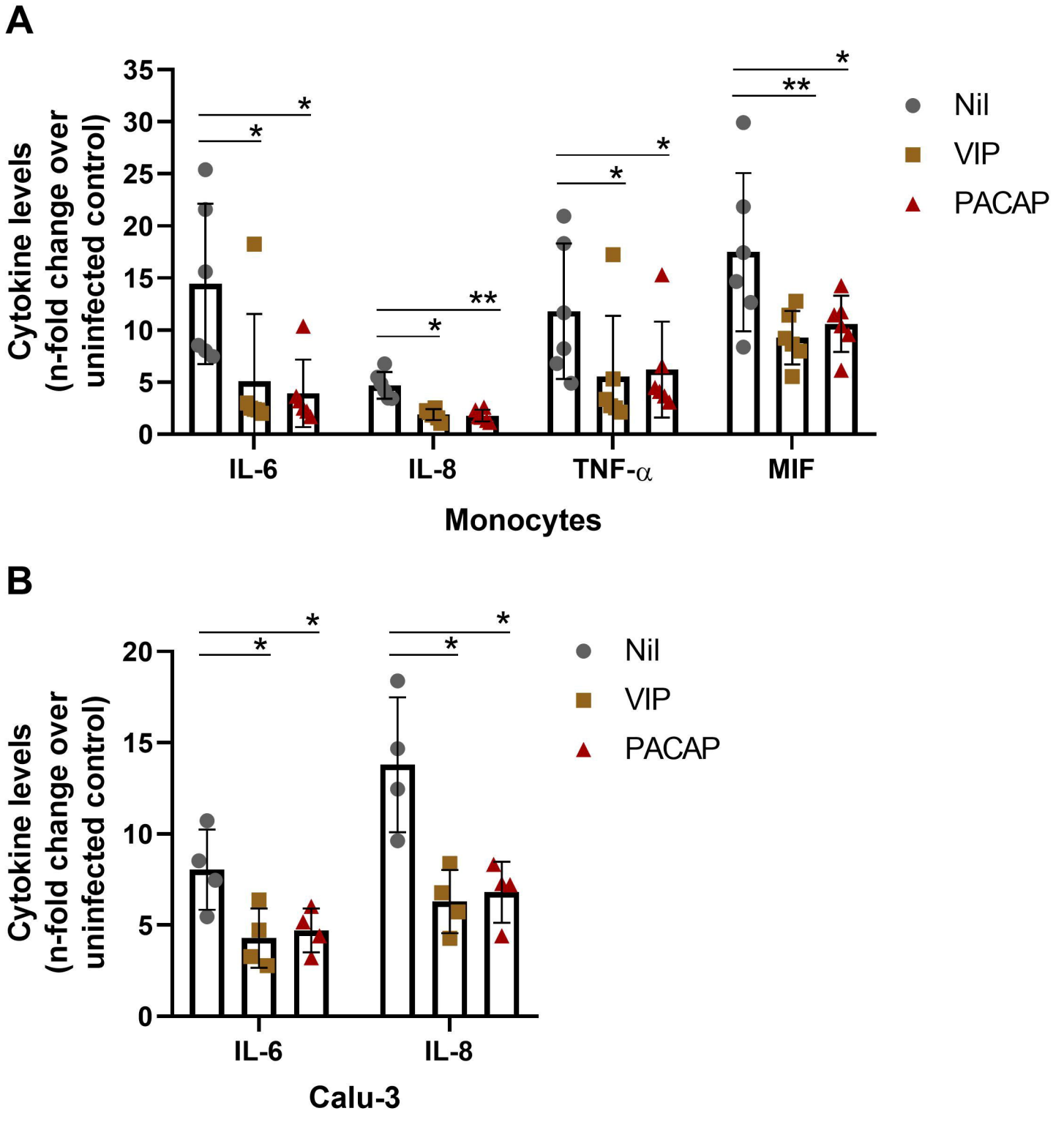
A
Cytokine levels (n-fold change over uninfected control)
35
30
25
20
15
10
5
0
*
*
**
*
*
*
**
IL-6
IL-8
TNF-α
MIF
Monocytes
Nil
VIP
PACAP
B
Cytokine levels (n-fold change over uninfected control)
20
15
10
5
0
*
*
*
*
IL-6
IL-8
Calu-3
Nil
VIP
PACAP

Figure 6

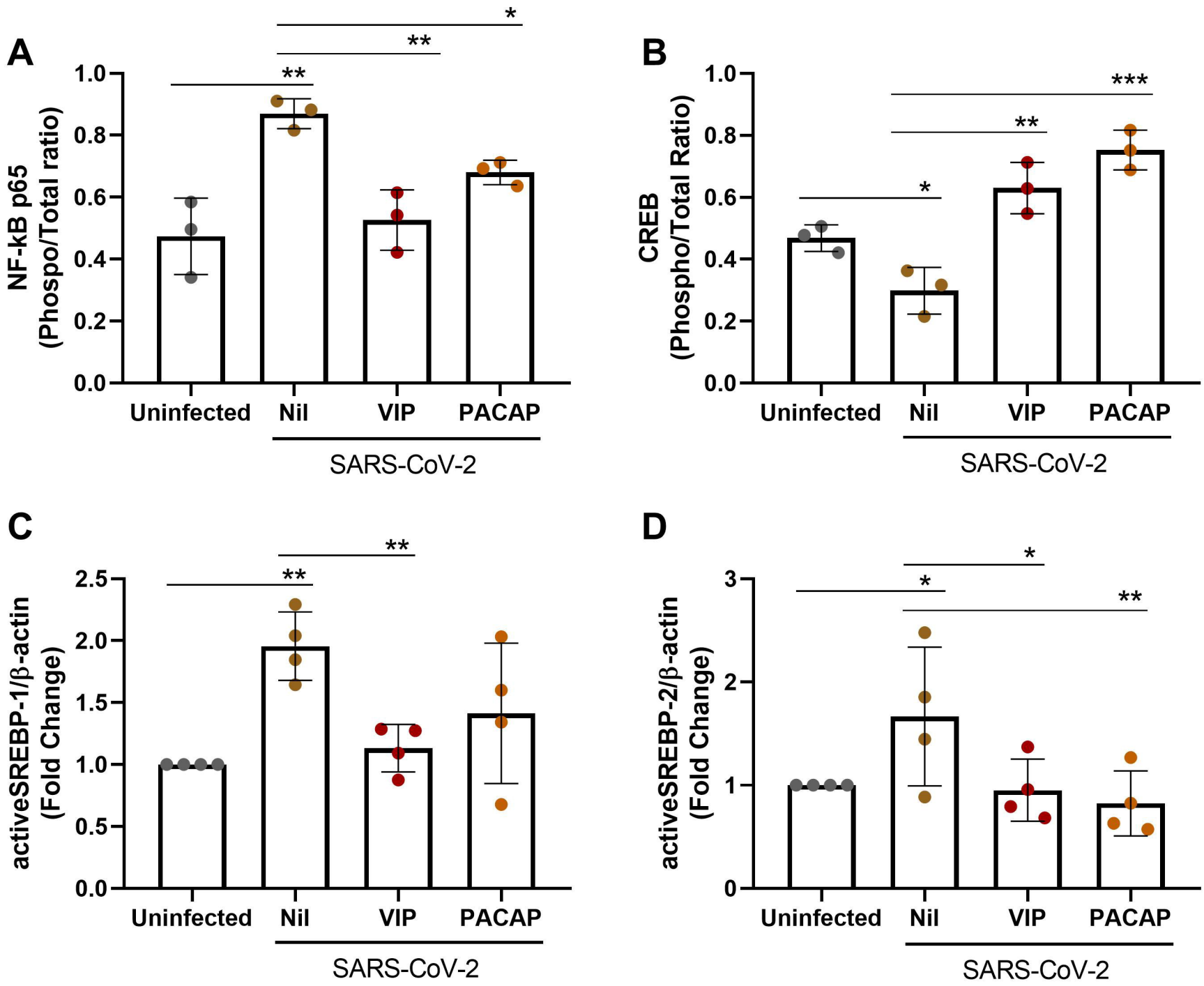
A
NF-kB p65
(Phospo/Total ratio)
1.0
0.8
0.6
0.4
0.2
0.0
**
**
*
Uninfected
Nil
VIP
PACAP
SARS-CoV-2
B
CREB
(Phospho/Total Ratio)
1.0
0.8
0.6
0.4
0.2
0.0
***
**
*
Uninfected
Nil
VIP
PACAP
SARS-CoV-2
C
activeSREBP-1/β-actin
(Fold Change)
2.5
2.0
1.5
1.0
0.5
0.0
**
**
Uninfected
Nil
VIP
PACAP
SARS-CoV-2
D
activeSREBP-2/β-actin
(Fold Change)
3
2
1
0
*
*
**
Uninfected
Nil
VIP
PACAP
SARS-CoV-2

Figure 7

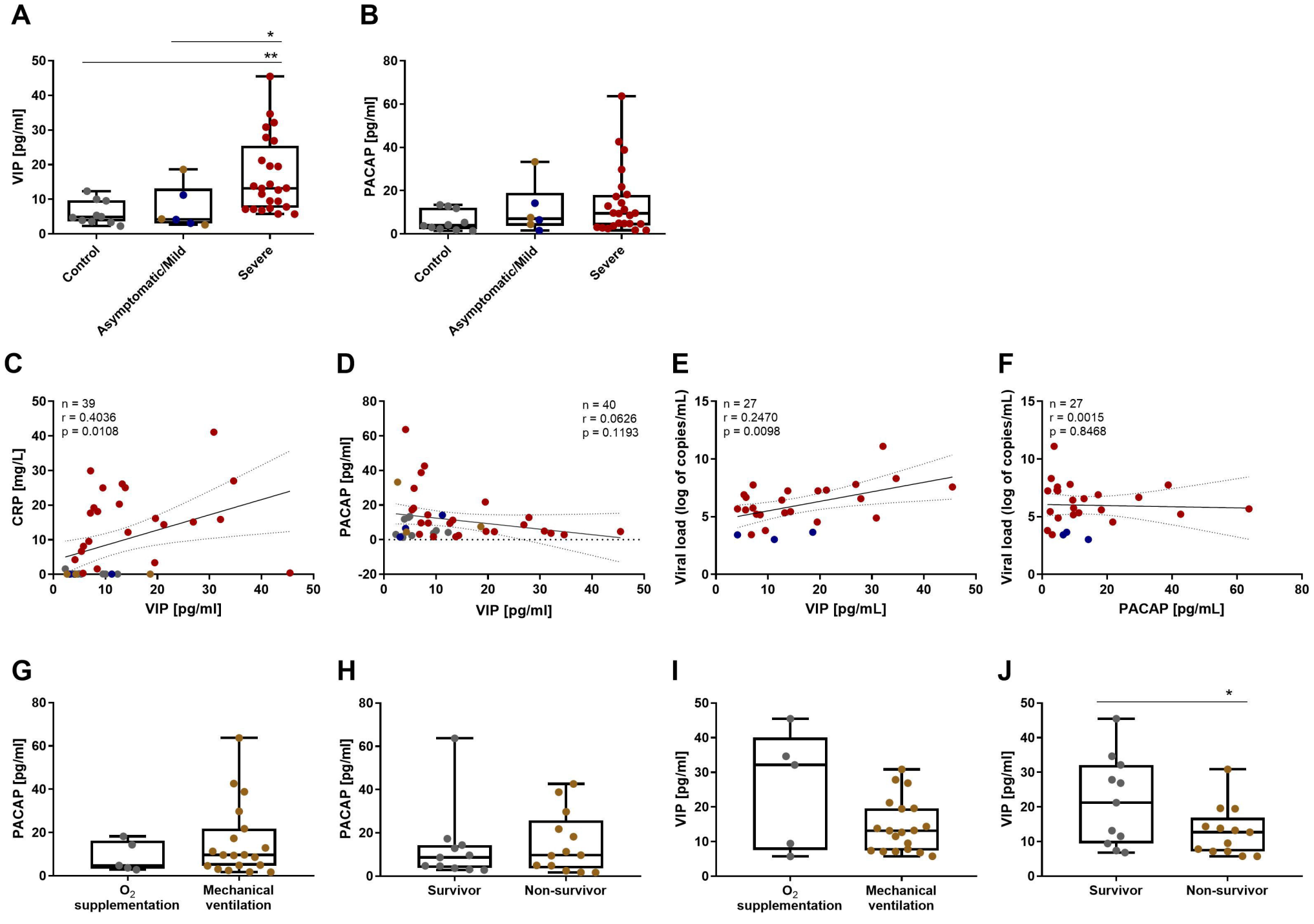
A
B
VIP [pg/ml]
PACAP [pg/ml]
Control
Asymptomatic/Mild
Severe
*
**
C
D
E
F
n = 39
r = 0.4036
p = 0.0108
CRP [mg/L]
VIP [pg/ml]
n = 40
r = 0.0626
p = 0.1193
PACAP [pg/ml]
n = 27
r = 0.2470
p = 0.0098
Viral load (log of copies/mL)
VIP [pg/mL]
n = 27
r = 0.0015
p = 0.8468
PACAP [pg/mL]
G
H
I
J
O2 supplementation
Mechanical ventilation
Survivor
Non-survivor